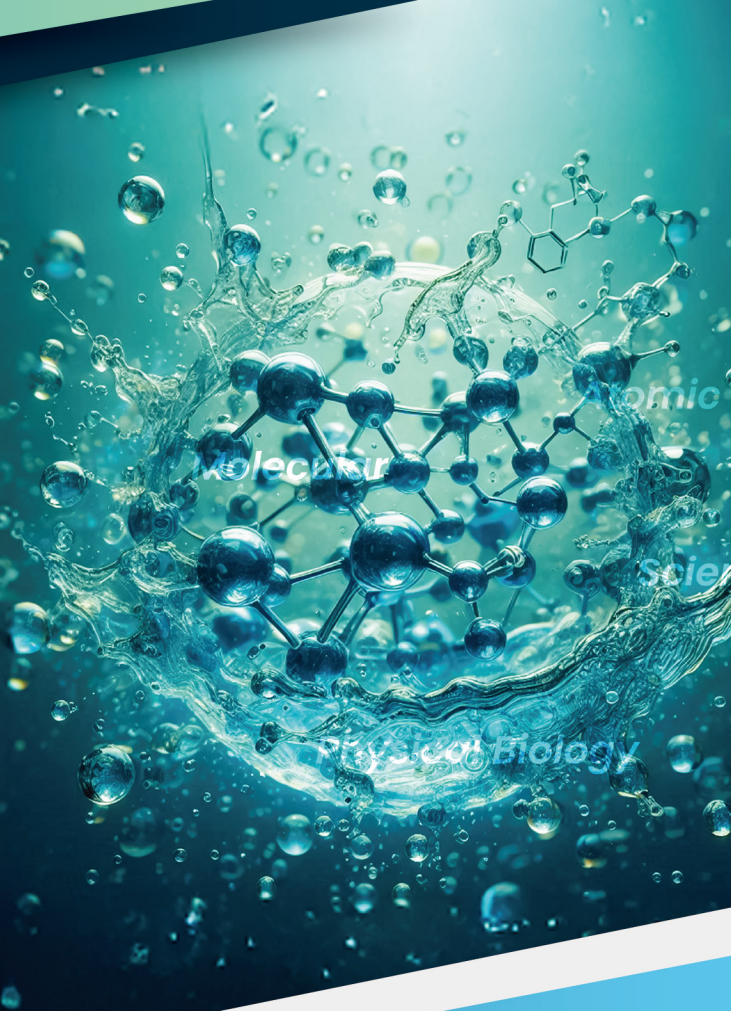


# INY 2025

## IAMS-NTNU-YCU

### AUTUMN WORKSHOP

# 2025





**AUGUST 27**  
**2025**

# ABSTRACT BOOK

## CONTACT US

 **Ms. Bonnie Lin** (Secretary)

 +886-2-23624928

 C. T. Chang Memorial  
Hall & Rm 504,  
Institute of Atomic and  
Molecular Sciences,  
Academia Sinica

# INY IAMS-NTNU-YCU

## 2025 AUTUMN WORKSHOP 2025



8 C. T. Chang Memorial Hall & Rm 504,  
Institute of Atomic and Molecular Sciences, Academia Sinica

Aug 27,  
2025

### Program

08:30 ~ 09:00	Registration
09:00 ~ 09:30	Start the meeting with an icebreaker Dr. Tsy-Yan Yu
Session A Chair : Prof. Masanori Tachikawa	
09:30 ~ 09:43	Yi-Shan Wu (IAMS) Investigation of methionine metabolism in coccolithophore by in situ light-coupled NMR spectroscopy
09:43 ~ 09:56	Yuta Hamamoto (YCU) Mass spectrometry of dimethyl sulfide oxidation products formed in atmospheric pressure corona discharges
09:56 ~ 10:09	Ai-Phuong Nguyen (IAMS) Short-wave near infrared hyperspectral imaging for single-wall carbon nanotube-based biosensors
10:09 ~ 10:22	Takaaki Mukai (YCU) Studies on the N-terminal-tryptophan-specific dual modification of peptides
10:22 ~ 10:35	Ayama Tokuyasu (YCU) Force propagation inside a living cell
10:35 ~ 10:55	Short break and connection check for online speakers Group photo session
Session B Chair : Prof. Masashi Tachikawa	
10:55 ~ 11:08	Miina Suzuki (YCU) Morphology of protein crystals grown in hydrogel
11:08 ~ 11:21	Taiga Ohnishi (YCU) Fluorescently labeled long-chain polyamines; synthesis and membrane permeability
11:21 ~ 11:34	Suguru Ushioda (YCU) Dynamics of Charged Particles Near a Rotating Bacterial Flagellum: A Simulation Study
11:34 ~ 11:47	Ryota Orie (YCU) Structural response of microtubule and actin cytoskeletons to direct intracellular load
11:47 ~ 12:00	Tomoyo Nishigaki (YCU) Modeling protein domain formation on the endoplasmic reticulum in eukaryotic cells
12:00 ~ 13:00	Lunch
13:00 ~ 14:30	Poster session
14:30 ~ 14:40	Session transition and poster area clean-up
Session C Chair : Prof. Ming-Kang Brad Tsai	
14:40 ~ 14:53	Miu Ashiba (YCU) Theoretical Analysis of Positron Binding to Hydrocarbons
14:53 ~ 15:06	Takumi Naito (YCU) Theoretical study of tin perovskite surface defects based on first-principles calculations
15:06 ~ 15:19	Fizza Sabbar (IAMS) Development of a Predictive Machine Learning Framework for Guiding Stereoselective Glycosylation
15:19 ~ 15:32	Hsin-Chen Lin (NTNU) First-Principle Simulation Study of CO <sub>2</sub> Reduction by Bi(III) Oxide Nanoparticle
15:32 ~ 15:50	Break
Session D Chair : Prof. Huan-Yu Ku	
15:50 ~ 16:03	Shuo-Yun Chang (IAMS) Direct growth of continuous Carbon Nitride film by thermal vapor deposition for photocatalytic applications
16:03 ~ 16:16	Shih-Chieh Chen (NTNU) Photoelectric Interaction in Micro-LED: Correlating PL Response with Circuit Conditions
16:16 ~ 16:29	Chun-Wei Chou (IAMS) Electrodeposited biocompatible Fe-Mo/CP electrode catalyst for efficient CO <sub>2</sub> fixation by integrating hydrogenotrophic bacterium <i>Ralstonia eutropha</i> H16
16:29 ~ 16:42	Somboon Fongchaiya (IAMS) Incommensurate Charge Density Wave Order in Dirac Nodal-Line Semimetals of GdSb <sub>0.7</sub> Te <sub>1.3</sub>
16:42 ~ 16:55	Muhammad Yusuf Fakhri (IAMS) High-performance thermoelectric cooling via strong anisotropy in earth-abundant tin sulfide
16:55 ~ 17:08	Yu-Chiao Chan (NTNU) Temperature-Dependent Valley Polarization of MoS <sub>2</sub> /Graphene Heterostructure by Resonant Polarization-Resolved PL Spectroscopy
17:08 ~ 17:45	Closing NTNU Representative YCU Representative IAMS Representative Award Ceremony
17:45 ~ 18:00	Break
18:00	Banquet

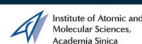
INY 2025  
Website





# INY IAMS-NTNU-YCU

## 2025 AUTUMN WORKSHOP 2025



8 C. T. Chang Memorial Hall & Rm 504,  
Institute of Atomic and Molecular Sciences, Academia Sinica

Aug 27,  
2025

### List of Poster Presentations

No.	Name	Poster Title
1	Ying-Xin Li	Chemical Modulation of Magnetic Phase Transitions in One-Dimensional Covalent Organic Frameworks
2	Hung-Hsi Tsai	Tailoring C <sub>3</sub> N <sub>4</sub> Nanotubes with Metals for Efficient CO Electroreduction to C <sub>1</sub> /C <sub>2</sub> Products
3	Sih-Ling Hsu	Strain-Modulated Electrocatalytic Activity of Fe-Decorated g-C <sub>3</sub> N <sub>4</sub> Surfaces
4	Zi-Xuan Tang	Edge Morphology Control on the Topological Structures and Magnetic Properties of Chiral Graphene Nanoribbons
5	Shu-An Shih	Peptide-based AIE fluorescent tag for detecting the amyloid formation by islet amyloid polypeptide
6	Cheng-Wei Tsai	Enhancing Equivariant Flow Matching for 3D Structure Generation with the Extended Features
7	Po-Chun Cheng	Investigating Soluble Protein Tags for Calcitonin Aggregation Inhibition
8	Yun-Hsuan Chen	Thermoresponsive Dual-Functional Gelatin Hydrogels for Inhibition of Human Calcitonin Amyloid Formation
9	Yu-Hsuan Chang	Investigating azide-alkyne cycloaddition in the presence of TFE to create stablized helical DM hCT fragment for inhibition of calcitonin amyloid
10	Wei-Fan Hsu	Rational Design of hIAPP Variants with Potent Antibacterial Activity through Targeted Arginine Substitutions
11	Yu-Rong Chen	A Computational Study on CO <sub>2</sub> Carboxylation of Aromatic and Aliphatic Terminal Alkynes Catalyzed by Lanthanide Amide Complexes
12	Yumnam Nganθοingnabhi	Computational Investigation of the Regioselective γ-Insertion of Alkynyl Carbenes into O-H Bonds: Mechanistic Insights and Selectivity Control.
13	Yi-Ning Wang	Bismuth-Based Metal-Organic Framework with Oxidoreductase-Like Activity for Hexavalent Chromium Detection
14	Yi-Fan Chiu	Photoluminescence and Raman characterization of monolayer MoS <sub>2</sub> under twisted and circularly polarized light
15	Ju-Yi Huang	Chemical Vapor Deposition Synthesis of 3R-stacked Molybdenum Disulfide for ferroelectric tunnel junction transistors
16	Shao-Quan Chang	Magnetic Field Driven Domain Evolution in van der Waal Material Fe <sub>3</sub> GaTe <sub>2</sub>
17	Cheng-Ying Hsiao	Graphene-Protected Interfaces in Chiral Perovskite/Cobalt Hybrid Structures
18	Shuo-Cheng Tsao	Raman and ARPES Characterization of Black Phosphorus for Contact Metal Optimization in FET Devices
19	Shih-Chia Peng	Interface Trap Reduction and Channel Optimization in 2D FETs through Dielectric and Work Function Engineering
20	Wei-Cheng Chen	Enhanced Synaptic Memory Window and Linearity with Laguerre-Gaussian Beam
21	Yi-Chun Chen	Exploring Dark Exciton in WSe <sub>2</sub> Through Orbital Angular Momentum Light
22	Hsin-Sung Chen	Pressure-Tunable Magnetism in 2D Ferromagnetic Fe <sub>3</sub> GaTe <sub>2</sub> via Local AFM Indentation
23	Tzu-Han Chang	Photoluminescence of MoS <sub>2</sub> on Platinum Substrate
24	Shuo-Yu Tseng	Photoresponse and Trap-State Effects in Monolayer MoS <sub>2</sub> Phototransistors Under Low-Power Illumination
25	Chun-Ting Wu	Emission Current Stability of Single-Atom Electron Sources
26	Jui-Po Chen	Effects of Dielectric Mismatch-Induced Lateral Heterojunctions and Annealing on the Optical Properties of WS <sub>2</sub>
27	Sumangaladevi Koodathil	Mapping Local Electrochemical Responses of 2D TMDCs Using AFM-SECM
28	Chimdessa Gashu Feyisa	Harnessing Non-Hermiticity for Fast GHZ- and W-state Generation in Superconducting Qubits
29	Pritam Sardar	Effect of Defects on Electronic and Magnetic Properties in NiPS <sub>3</sub> Layers
30	Che-Wei Chang	Absolute Line Strength Measurements of HO <sub>2</sub> v1 and v2 Fundamental Bands
31	Varad Modak	Tuning the selectivity of Electrocatalytic CO <sub>2</sub> Reduction by Engineering the Coordination Environment of Bi SACs
32	Yu-Sheng Yu	Modulatable melanocyte dedifferentiation through niche prolactin sensing controls seasonal coat color switch in Djungarian hamster
33	Lily Maysari Angraini	Exploring the influence of S/Cl sites' mixing on the lithium diffusion behaviors of Li <sub>x+6</sub> PS <sub>4</sub> (S/Cl)
34	I Gusti Ngurah Yudi Handayana	Suppression of quantum correlations in a clean-disordered atom-nanophotonic interface
35	Cao Hieu Dong	Quantum-Derived Neural Network Potentials Elucidate Peptide Bond Isomerization, Charge State Stability, and Secondary Structure Distribution in Short Oligopeptides of Glycine, Alanine, and Sarcosine

INY 2025  
Website



# Investigation of methionine metabolism in coccolithophore by in situ light-coupled NMR spectroscopy

Yi-Shan Wu,<sup>a,b,c</sup> Li-Kang Chu,<sup>d</sup> Tsyr-Yan Yu,<sup>a,b,c</sup>

<sup>a</sup>Institute of Atomic and Molecular Sciences, Academia Sinica, Taipei 106923, Taiwan

<sup>b</sup>International Graduate Program of Molecular Science and Technology, National Taiwan University No. 1, Sec. 4, Roosevelt Rd., Daan Dist., Taipei, 106923, Taiwan

<sup>c</sup>Molecular Science and Technology Program, Taiwan International Graduate Program (TIGP), Academia Sinica No. 1, Sec. 4, Roosevelt Rd., Daan Dist., Taipei, 106923, Taiwan

<sup>d</sup>Department of Chemistry, National Tsing Hua University, No. 101, Sec. 2, Kuang-Fu Road, Hsinchu, 300044, Taiwan  
e-mail: d09551002@g.



## ABSTRACT

Coccolithophores play critical roles in the global carbon and sulfur cycles. They contribute to the carbon cycle through photosynthesis and calcification, and to the sulfur cycle by producing dimethylsulfoniopropionate (DMSP). Despite their ecological importance, the details and dynamics of methionine metabolism in coccolithophores remain poorly understood. Here, we introduce an *in situ* light-coupled nuclear magnetic resonance (NMR) spectroscopy setup to monitor methionine metabolism directly in coccolithophore cultures under varying environmental conditions. Combining *in situ* light-coupled NMR spectroscopy and <sup>13</sup>C magic angle spinning (MAS) spectroscopy, we observed that coccolithophores can uptake methionine and convert it into 4-methylthio-2-oxobutyrates (MTOB), which is subsequently secreted into the culture medium, while DMSP was detected only intracellularly. Furthermore, environmental factors such as elevated temperatures at 24.8 °C, which is 6.8 °C higher than the typical growth temperature for coccolithophores, and darkness accelerated methionine consumption but reduced its incorporation into proteins and its conversion into MTOB, suggesting a shift toward alternative metabolic pathways under stress. In contrast, seawater acidification had minimal effects on methionine metabolism. These findings provide new insights into how environmental conditions influence sulfur metabolism in coccolithophores, with potential consequences for their ecological functioning under future climate scenarios.

## References

1. Wu, Y. S., Chu, L. K., & Yu, T. Y. (2025). Investigation of Methionine Metabolism in Coccolithophore by In Situ Light-Coupled Nuclear Magnetic Resonance Spectroscopy. *The Journal of Physical Chemistry Letters*, 16, 5800-5805.



# Mass spectrometry of dimethyl sulfide oxidation products formed in atmospheric pressure corona discharges

**Yuta Hamamoto, Kanako Sekimoto**

Graduate School of Nanobioscience, Yokohama City University  
e-mail: n255221b@yokohama-cu.ac.jp



## ABSTRACT

Dimethyl sulfide (DMS) is a volatile sulfur compound released from the ocean and is known as the scent of the sea. After DMS is released into the atmosphere and oxidized, it turns into sulfate aerosols. They act as cloud condensation nuclei and will increase cloud reflectivity. It has been considered that the emission of DMS into the atmosphere could prevent global warming by reducing solar radiation to the earth<sup>1)</sup>. The pathways that DMS is converted to sulfate aerosols depend on many environmental factors such as temperature, humidity, and oxidants in the atmosphere, and therefore the detailed reaction mechanism is not fully understood.

Based on these backgrounds, we performed fundamental studies to analyze various oxidation products of DMS using an atmospheric pressure corona discharge ionization mass spectrometry (APCDI-MS). We will discuss the relationship between oxidants and the formation of oxidation products.

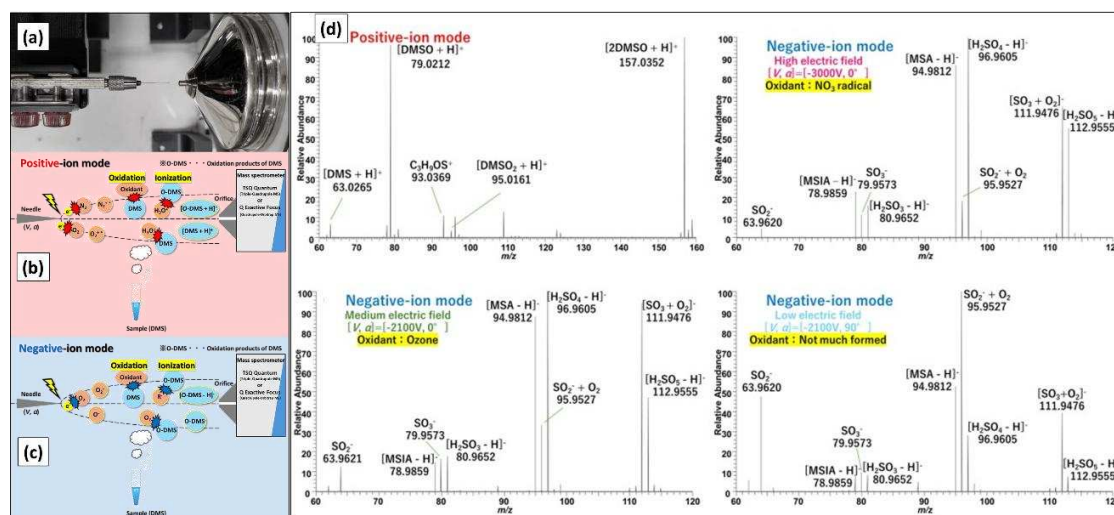


Figure 1. (a) Photo of APCDI ion source. (b)-(c) APCDI ionization mechanisms. (d) Positive- and negative-ion APCDI mass spectra of DMS.

## References

1. R. Charlson, J. Lovelock, M. Andreae, and S. Warren. **Oceanic phytoplankton, atmospheric sulphur, cloud albedo and climate**, *Nature*, Vol.326, 655-661 (1987).

# Short-wave near infrared hyperspectral imaging for single-wall carbon nanotube-based biosensors

**Ai-Phuong Nguyen<sup>1,2,3</sup>, Ching-Wei Lin<sup>1,\*</sup>**

<sup>1</sup>*Institute of Atomic and Molecular Sciences, Academia Sinica, Taipei 10617, Taiwan*

<sup>2</sup>*Taiwan International Graduate Program, Academia Sinica, Taipei 10617, Taiwan*

<sup>3</sup>*Department of Chemistry, National Tsing Hua University, Hsinchu 300044, Taiwan*

*e-mail: nguyenthiaiphuong.kl3cla@gmail.com*

## ABSTRACT

Hyperspectral imaging is an advanced approach that allows visualization to examine the fluorescence and spectral variations of nanoparticles simultaneously in single-particle resolution. Among nanomaterials, semiconducting single-wall carbon nanotubes (SWCNTs) have emerged as exceptional candidates for biosensor applications, especially in the short-wave near-infrared (SWIR) range. This range offers significant advantages, including high tissue transparency, low scattering and autofluorescence, and photostable fluorescence, making it highly suitable for biomedical imaging. Chirality-sorted individualized SWCNTs provide distinct fluorescence emission peaks in the SWIR range, enabling multiplexed detection across multiple channels. This work demonstrates the utility of SWCNTs as tunable fluorescent probes for SWIR hyperspectral imaging studying the nanotube behaviors, and interaction of the single nanotubes in the cell. SWCNTs are chemically modified to introduce three types of  $sp^3$  defects, resulting in emission peaks at 1094 nm, 1138 nm, and 1260 nm. Each antibody will be uniquely labeled with SWCNTs emitting at a specific wavelength, enabling multiplexed emitter channels. The covalent conjugation nanotubes with antibodies will enable precise, stable, and multiplexed fluorescence emitters. The successful defects will be verified through 2D fluorescence spectroscopy and visualized in the hyperspectral imaging. The development of advanced imaging modalities to probe SWCNT spatial distribution and spectral property simultaneously will provide a robust platform for SWCNT-based biosensors.



# Studies on the N-terminal-tryptophan-specific dual modification of peptides

**Takaaki Mukai, Raku Irie, Masato Oikawa**

Affiliation (Yokohama City University)

e-mail: (n255226g@yokohama-cu.ac.jp)

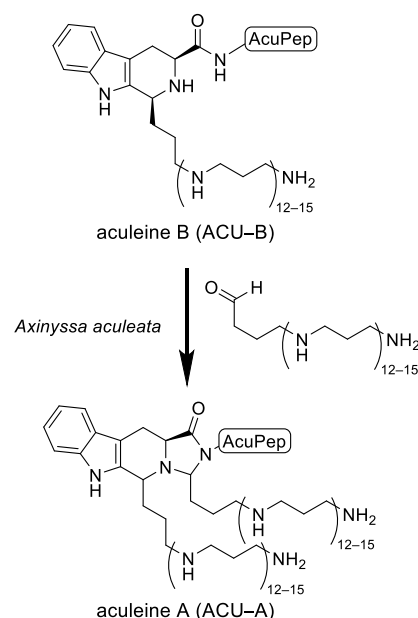


## ABSTRACT

Selective N-terminal modification of peptides is a valuable strategy for introducing functional diversity, and dual modifications are particularly attractive for overcoming the limitations of single modifications. Here, we report a novel dual modification reaction targeting the N-terminal tryptophan residue, inspired by the post-translational modifications observed in the marine natural product aculeine A (ACU-A).

ACU-A, isolated from the sponge *Axinyssa aculeata*, consists of a polypeptide (Trp–AcuPep) post-translationally modified by two long-chain polyamines (LCPAs), though its detailed structure remains to be elucidated. Previously, we elucidated the structure of the related compound aculeine B (ACU-B), bearing a single LCPA modification. We then proposed a putative chemical structure for ACU-A featuring a unique dual modification at the N-terminal Trp.

To investigate the underlying dual modification reaction, we conducted model experiments using a dipeptide (H–Trp–Tyr–NH<sub>2</sub>) and excess aldehydes. The reaction yielded a tetracyclic product via a Pictet–Spengler reaction and 4-imidazolidinone ring formation. Similar results were obtained with H–Trp–Ala–NH<sub>2</sub>, indicating the general applicability of the reaction to Trp-terminated peptides. Further optimization of solvents and acid catalysts improved both reactivity and stereoselectivity.



## References

1. S. Matsunaga, et al., **ChemBioChem**, 12, 2191–2200 (2011).
2. R. Irie, et al., **J. Nat. Prod.**, 84, 1203–2200 (2021).

# Force propagation inside a living cell

**Ayama Tokuyasu<sup>1</sup>, Hirokazu Tanimoto<sup>1</sup>**

<sup>1</sup>Grad. Sch. Nanobioscience, Yokohama city university, Kanagawa, Japan  
e-mail: n255301e@yokohama-cu.ac.jp



## ABSTRACT

Mechanical forces produced in living cells are essential in various cell-biological processes including cell motility and division. In multicellular systems, intracellular stresses were calculated using monolayer stress microscopy and Bayesian inversion stress microscopy<sup>1,2</sup>. However, it is difficult to map the propagation of forces inside the cell using these techniques.

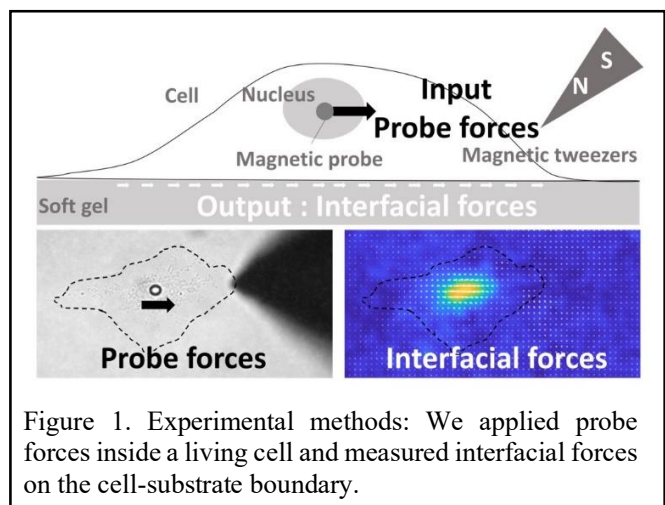


Figure 1. Experimental methods: We applied probe forces inside a living cell and measured interfacial forces on the cell-substrate boundary.

We established a new approach for mapping the propagation of mechanical forces in the cytoplasm of adherent cells. By combining intracellular magnetic tweezers with traction force microscopy, we investigated how mechanical forces applied to the cell propagated in the cell to the cell-substrate boundary. We found that the mechanical forces partly spread in the cytoplasm during propagation. We also quantified intracellular stresses from the force balance between interfacial forces. In the presentation, we will show these results and discuss about the features of the propagated forces and the roles of cytoskeletons in the stress propagation.

## References

1. Tambe, Dhananjay T., et al. "**Monolayer stress microscopy: limitations, artifacts, and accuracy of recovered intercellular stresses.**", *PloS one*, e55172 (2013).
2. Nier, Vincent, et al. "**Inference of internal stress in a cell monolayer.**", *Biophysical journal* 110.7, 1625-1635 (2016).



# Morphology of protein crystals grown in hydrogel

**Miina Suzuki, Ryo Suzuki, Masaru Tachibana**

Graduate school of Nanobioscience, Yokohama City University, Japan

e-mail: n245213d@yokohama-cu.ac.jp



## ABSTRACT

The growth of high-quality protein crystals is a prerequisite for the structure analysis of proteins by X-ray diffraction. Several methods have been developed to obtain such high-quality crystals. One of them is the gel method. The gel method is expected to promote the growth of high-quality crystals by suppressing convection. Previous studies showed that protein crystals grown in gel were more resistant to X-ray and handling damage, while maintaining structural analysis accuracy comparable to pure protein crystals<sup>1</sup>. We also reported that gel-incorporated protein crystals had ten times greater fracture strength<sup>2</sup>. While the physical properties of the crystals grown in gel have been studied, their growth mechanism remains unclear. Elucidating the growth mechanism could lead to the establishment of methods for producing high-quality crystals and may also contribute to drug discovery research and the development of novel composite materials.

In this study, we obtain protein crystals in various concentrations of gel and observed using an optical microscope. Tetragonal hen egg-white lysozyme (T-HEWL) crystals ( $P4_32_12$ ,  $a = b = 7.91$  nm,  $c = 3.79$  nm) were prepared by allowing the mixture to stand the mixture of protein solution, sodium chloride, sodium acetate (pH 4.5), and agarose gel at pH4.5. Agarose gel was prepared at concentrations ranging from 0.1 to 5 wt.%. As a result, crystal growth was successfully achieved at all gel concentrations. Remarkably, as gel concentration increased, morphology has changed. In general, crystals grow in a way that leads to thermodynamic stability. Due to the anisotropy of molecular structure and intermolecular interactions, they exhibit polyhedral shapes. The typical shape of T-HEWL crystal is composed of four hexagonal faces and eight rhombic faces. The crystal shape was typical at gel concentration of 1.5 wt.% and below. However, the aspect ratio of  $\langle 001 \rangle$  and  $\langle 110 \rangle$  directions increased. On the other hand, crystal morphology has changed dramatically at gel concentration of 2.0 wt.% and above. A concavity was observed at the center of the crystal face, and the  $\{011\}$  and  $\{101\}$  faces became curved, causing the boundary between these faces to disappear. Furthermore, surface curvature became more pronounced, and ellipsoidal or spherical crystals were observed at higher gel concentrations. To identify the crystal structure of spherical crystals, X-ray structural analysis was performed. As a result, the spherical crystals grown in 5 wt.% gel exhibited the same lattice constants as those of pure T-HEWL crystals. This behavior is thought to be caused by the gel network equalizing the free energy, leading to the formation of spherical crystals. In the presentation, the details of the morphological changes and their investigation are discussed.

## References

1. S. Sugiyama et al., J. Am. Chem. Soc. 134, 5786-5789 (2012).
2. R. Suzuki et al., ACS Appl. Bio Mater. 6, 965-972 (2023).

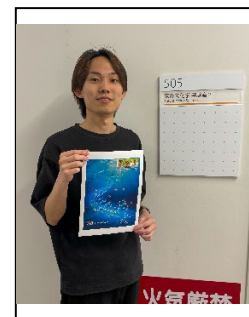
# Fluorescently labeled long-chain polyamines; synthesis and membrane permeability

**Taiga Ohnishi,<sup>1</sup> Raku Irie,<sup>1</sup> Hiroki Sato,<sup>1</sup>  
Makoto Inai,<sup>2</sup> Toshiyuki Kan,<sup>2</sup> Shouichi Higashi,<sup>1</sup>  
Masato Oikawa<sup>1</sup>**

<sup>1</sup> School of Nanobioscience, Yokohama City University

<sup>2</sup> School of Pharmaceutical Sciences, University of Shizuoka

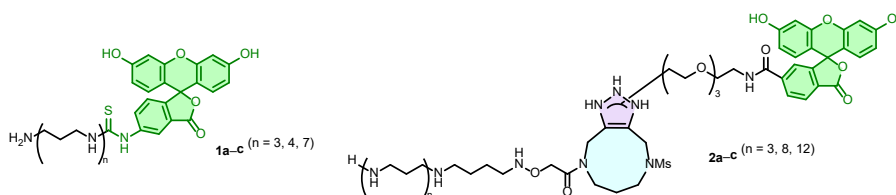
e-mail: n245206d@yokohama-cu.ac.jp



## ABSTRACT

Aculeines, polyamine-polypeptide conjugates isolated from an Okinawan marine sponge *Axinyssa aculeata*, exhibit potent cytotoxicity by penetrating cell membranes and entering the nucleus.<sup>1</sup> In our previous study, neither the polypeptide nor the LPCA moiety exhibits cytotoxicity, whereas the LPCA (12-mer) alone exhibited membrane permeability. This observation suggests that the polypeptide, being the cytotoxic entity, is delivered into cells by the LPCA moiety, thereby showing the cytotoxicity. To verify the hypothesis, fluorescently labeled LCPAs (FL-LCPAs) with diverse chain lengths were prepared and their membrane permeability was evaluated.

The FL-LCPAs **1a–c** and **2a–c** were synthesized using our previously established synthetic method.<sup>2</sup> From cellular uptake experiments, the membrane permeability of the synthesized FL-LCPAs was found to increase in a chain length-dependent manner, with **2c** (12-mer) exhibiting the highest level of intracellular fluorescence. These findings may show that the sponge is strategically using 12-mer or even longer LCPAs with high membrane permeability for the biological defense.



## References

- [1] (a) S. Matsunaga et al. *ChemBioChem* **2011**, *12*, 2191. (b) H. Watari et al. *Chem. Lett.* **2023**, *52*, 185. [2] (a) T. Ohnishi et al. *Bull. Chem. Soc. Jpn.*, **2025**, *98*, uoaf014. (b) T. Ohnishi et al. IAMS-NTNU-YCU Autumn Workshop 2024, No. 10.



# Dynamics of Charged Particles Near a Rotating Bacterial Flagellum: A Simulation Study

**Suguru Ushioda, Masashi Tachikawa**

*Grad. Sch. of Nanobioscience, Yokohama City Univ.*

e-mail: n245204b@yokohama-cu.ac.jp



## ABSTRACT

Bacteria swim inside cells, where there are many substances with electrical polarity around their flagella. Recently, it has been reported that the flagella themselves carry a negative charge [1]. Therefore, understanding how the dynamic distribution of charged substances changes due to electrostatic interactions with the flagella is a highly interesting topic, both for its possible effects on bacterial swimming efficiency and as a problem in nonequilibrium physics. In this study, we modeled a rotating flagellum as a negative charge performing uniform circular motion in a two-dimensional plane, and we simulated the time evolution of the distribution of positive charges around it by numerically solving the Poisson–Nernst–Planck (PNP) equations (see figure). When the rotation radius of the negative charge was fixed to the Debye length, the simulation revealed that the concentration profile of positive charges varied with the angular velocity of the negative charge: exhibiting a single-peak pattern at low angular velocities, a dome-shaped pattern at intermediate velocities, and a donut-shaped pattern at high velocities. This indicates that the combination of angular velocity and rotation radius of the negative charge determines the distribution of counterions.

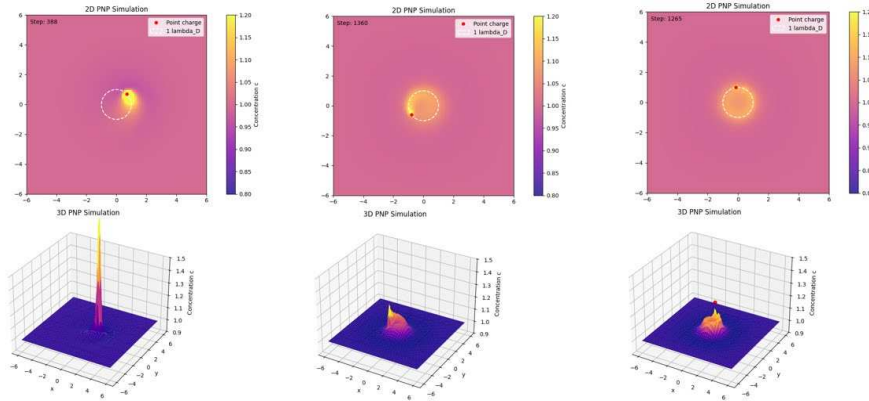


**Figure.** Positive charge concentration distributions around a rotating negative charge (red dot) with its rotation radius fixed at the Debye length (white dotted line), for three different angular velocities: low (left), medium (center), and high (right). Yellow regions indicate areas with high concentrations of positive charges.

## References

[1] Fields, J. L. *et al.* Structural diversity and clustering of bacterial flagellar outer domains, *Nat. Commun.*, **15**, 9500 (2024).

# Structural response of microtubule and actin cytoskeletons to direct intracellular load

**Ryota Orie, Hirokazu Tanimoto**

Department of Science, Yokohama City University  
[n235303f@yokohama-cu.ac.jp](mailto:n235303f@yokohama-cu.ac.jp)



## ABSTRACT

Microtubule and actin are the two major cytoskeletal polymers physically driving fundamental biological processes in the cell interior in eucaryotes. How microtubule and actin cytoskeletons respond to the loads is poorly understood. In this study, we directly applied perturbing intracellular forces to microtubule and actin cytoskeletons and quantitatively evaluated how these cytoskeletons structurally respond to the loads [1]. We established a new ferrofluid-based intracellular magnetic tweezers and observed that in a creep experiment,  $\sim 10$  nN loads displaced the microtubule-nucleus complex several micrometers away from the stationary position over 10-20 seconds and revealed that rheological properties of the microtubule complex primarily determined by filamentous actin. The deformation of the microtubules was largest at the load position and decayed toward the cell periphery. We found that the deformations of actin meshwork follow the same scaling of microtubules. This result suggests that the two cytoskeletal systems behave as an integrated elastic body. We then investigated shape dynamics of a single microtubule under the perturbing loads. The microtubules exhibited non-Euler buckling in response to compressed loads, suggesting that microtubules are enclosed within actin meshwork at the polymer scale. Lastly, we demonstrated that a point force localized in the cytoplasm propagates in actin meshwork and deforms a microtubule at a distance. Taken together, our results suggest that microtubule and actin cytoskeletons act as an integrated continuum in the cytoplasm in response to intracellular loads.

## References

1. Ryota Orie, Hirokazu Tanimoto; Structural response of microtubule and actin cytoskeletons to direct intracellular load. *J Cell Biol* 3 February 2025; 224 (2)



# Modeling protein domain formation on the endoplasmic reticulum in eukaryotic cells

**Tomoyo Nishigaki, Masashi Tachikawa**

Dept. of Materials System Science, Grad. Sch. of Nanobioscience,  
Yokohama City Univ.  
e-mail: n255218f@yokohama-cu.ac.jp



## ABSTRACT

Membrane traffic, the process by which macromolecules are transported within the cell by encapsulating them in vesicles, plays a crucial role in cellular functions and is essential for understanding the structures of the nervous system, immune system, and cancer development. As the endoplasmic reticulum (ER) serves a major hub in membrane traffic, the transport between the ER and the Golgi apparatus has been widely studied. However, the mechanism underlying the formation of ER exit sites (ERES), where transport vesicles are assembled, remains unclear. In this study, we focused on Sar1p and Sec23/24p, two key components of transport vesicles, and aimed to construct a mathematical model of ERES formation and validate its effectiveness. Model 1 successfully simulated the stable accumulation of Sec23/24p, but failed to capture the local accumulation of Sar1p observed in previous studies<sup>1</sup>. To address this, we introduced a Sar1p-Sec23/24p complex in Model 2, which showed Sar1p accumulation but could not replicate stable Sec23/24p clustering. These results highlight the complexity of ERES formation, and future models aim to more accurately reproduce experimental observations.

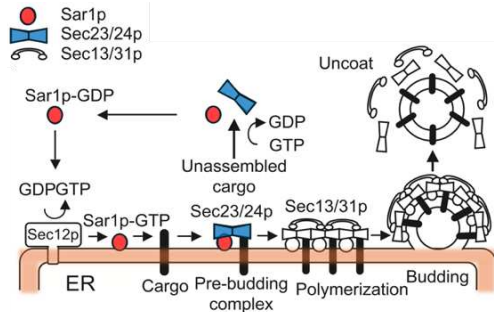


**Fig. 1** The process of vesicle formation (modified from <sup>2</sup>)  
Sar1p-GDP is converted to Sar1p-GTP by Sec12p, activating Sar1p. Sar1p-GTP undergoes a conformational change and binds to the ER membrane. Sec23/24p binds to Sar1p-GTP and cargo proteins, forming the pre-budding complex. Sec13/31p cross-links multiple pre-budding complexes, concentrating COPII and cargo at ERES. The COPII coat alters the ER membrane curvature, leading to budding and vesicle formation.

$$\begin{aligned}\frac{\partial u}{\partial t} &= \frac{K_0}{1 + \left(\frac{v+w}{t_0}\right)^{H_0}} - K_1 u - K_3 u + D_u \Delta u \\ \frac{\partial w}{\partial t} &= K_3 u - K_4 (v+w) w + D_w \Delta w \\ \frac{\partial v}{\partial t} &= K_4 (v+w) w - \frac{K_2}{1 + \left(\frac{v+w}{t_2}\right)^{H_2}} v + D_v \Delta v\end{aligned}$$

**Fig. 2** Model 2

This model used  $u$  as the concentration of Sar1p,  $w$  as Sar1p-Sec23/24p complex, and  $v$  as Sec23/24p.

## References

1. H. Iwasaki, T. Yorimitsu & K. Sato, *Journal of Cell Science*, 130, 2893-2902 (2017).
2. 佐藤健, *生物物理*, 47, 222-227 (2007).

# Theoretical Analysis of Positron Binding to Hydrocarbons

**Miu Ashiba<sup>1</sup>, Daisuke Yoshida<sup>2</sup>, Yukiumi Kita<sup>1</sup>,  
Tomomi Shimazaki<sup>1</sup>, Toshiyuki Takayanagi<sup>3</sup>,  
and Masanori Tachikawa<sup>1</sup>**

<sup>1</sup> Graduate School of NanoBioScience, Yokohama City University,  
Japan

<sup>2</sup> Department of Physics, Tohoku University, Japan

<sup>3</sup> Department of Chemistry, Saitama University, Japan

e-mail: [n245201f@yokohama-cu.ac.jp](mailto:n245201f@yokohama-cu.ac.jp)



## ABSTRACT

A positron, the antiparticle of an electron, is increasingly used in applications like cancer detection and identifying lattice defects. However, its detailed properties at the atomic and molecular level remain largely unknown. Positrons are known to form metastable positron compounds when interacting with atoms or molecules, and a key physical quantity characterizing these compounds is the positron affinity (PA), which represents the positron's binding energy<sup>1</sup>. Previous studies suggested a proportional relationship between polarizability and PA in short alkane chains, with saturation behavior indicated for longer chains<sup>2</sup>. Yet, this phenomenon is still poorly understood. Furthermore, there's a clear need for more research on longer chains of unsaturated hydrocarbons, such as alkenes and cycloalkanes. In this study, we systematically investigated the positron binding properties of hydrocarbons using calculations based on density functional theory (DFT) combined with the correlation polarization potential (CPP) model, an approach previously validated for such systems<sup>3,4</sup>.

As shown in Figure 1, the PA of long-chain alkanes increases with the carbon number up to approximately C20, beyond which it tends to saturate. Results for alkenes and other related compounds will be presented in detail on the day of the conference.

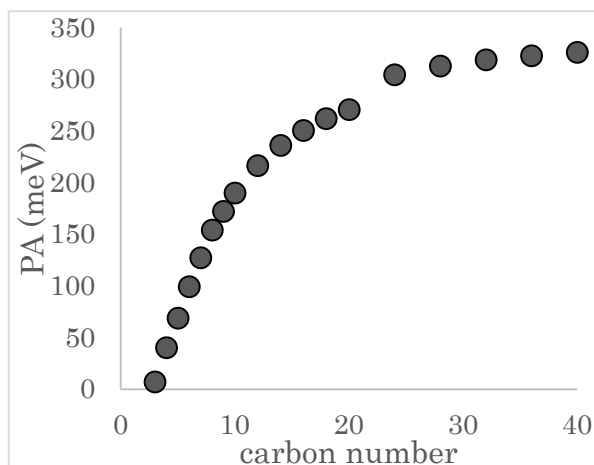


Figure 1. Relationship between the number of carbon in alkanes and PA

## References

1. G. F. Gribakin, J. A. Young, and C. M. Surko, **Rev. Mod. Phys.**, 82 2557 (2010).
2. J. R. Danielson *et al.*, **Phys. Rev. A**, 108, 032801(2023)
3. Y. Sugiura *et al.*, **J. Comput. Chem.** 41, 17 (2020).
4. D. Yoshida *et al.* **Phys. Chem. Chem. Phys.** 27, 12171-12181 (2025)

# Theoretical study of tin perovskite surface defects based on first-principles calculations

**Takumi Naito<sup>1</sup>, Makito Takagi<sup>1</sup>, Masanori Tachikawa<sup>1</sup>,  
Koichi Yamashita<sup>1</sup>, Tomomi Shimazaki<sup>1</sup>**

<sup>1</sup>Graduate School of Nanobioscience, Yokohama City University  
e-mail: n255302f@yokohama-cu.ac.jp

## ABSTRACT

Perovskite solar cells (PSCs) are strong candidates for next-generation solar cells. On the other hand, recombination centers formed by lattice defects in perovskites can supplement charge carriers and cause PCE degradation and hysteresis, so passivation approaches are used.<sup>1</sup> Formation of organic molecular films on crystal surfaces and interfaces is one such approach,<sup>2</sup> but the detailed mechanism is not clear. In this study, we performed a comprehensive analysis of surface defects in tin perovskite  $\text{MASnI}_3$  based on first-principles calculations to identify the defect species that cause carrier trapping and to analyze effective passivation molecules.

The results suggest that antisite defects  $\text{I}_{\text{Sn}}$  and atomic vacancies  $\text{V}_{\text{Sn}}$  are dominant defects in tin perovskite, and that carrier trapping originating from these defects can be improved by passivation with ethylenediamine (EDA).

## References

1. F. Gao, Y. Zhao, X. Zhang, J. You, **Adv. Energy Mater.** *10*(13), 1902650 (2020)
2. Y. Shao, Z. Xiao, C. Bi, Y. Yuan, J. Huang, **Nat. Commun.** *5*(1), 5784 (2014)



# Development of a Predictive Machine learning Framework for Guiding Stereoselective Glycosylation

**Fizza Sabbor<sup>[1,2,3]</sup> and Cheng-Chung Wang<sup>\*[1]</sup>**



<sup>1</sup>Institute of Chemistry, Academia Sinica, Taipei 115, Taiwan

<sup>2</sup>Department of Chemistry, National Tsing Hua University, Hsinchu 300, Taiwan

<sup>3</sup>Molecular Science and Technology (MST)- Taiwan International Graduate Program (TIGP)

e-mail: sabbor0001@gate.sinica.edu.tw

## ABSTRACT

Precise stereocontrol in glycosidic bond formation remains a central challenge in carbohydrate chemistry, limiting access to complex oligosaccharides and glycoconjugates. Here, we introduce a data-rich machine learning framework “*GlycoComputer 2.0*” for predicting and optimizing glycosylation stereoselectivity and efficiency. By parameterizing over 300 batch glycosylations with experimentally validated, and quantified descriptors—Relative Reactivity Value (RRV), Acceptor nucleophilic constant (Aka), and a newly developed statistical quantification index “*Environmental Factor impact Index (EFI)*”—the model captures the interplay of structure, reactivity, and conditions governing  $\alpha/\beta$ -selectivity. Employing a Random Forest algorithm, GlycoComputer 2.0 achieves high predictive accuracy, with  $R^2=0.90$  for  $\alpha$ -selectivity,  $R^2=0.79$  for yield, and RMSE=8%. Feature analysis reveals nucleophile reactivity and structure as dominant determinants, with solvent and temperature acting contextually. GlycoComputer 2.0 enables algorithm-guided optimization and reliable extrapolation to untested glycosylating agent–alcohol pairs, transforming stereoselective glycosylation from empirical trial-and-error into a predictive, data-driven process for carbohydrate synthesis and glycobiology.

# First-Principle Simulation Study of CO<sub>2</sub> Reduction by Bi(III) Oxide Nanoparticle

**Hsin-Chen Lin**

Department of Chemistry, National Taiwan Normal University, Taipei, Taiwan  
e-mail: 61342003s@gapps.ntnu.edu.tw

## ABSTRACT

Bismuth-based oxides have shown the potential in converting CO<sub>2</sub> to formate ions.<sup>1</sup> This study aims to computationally assess if bismuth trioxide, with its multiple valencies, can break the carbon-oxygen double bond of CO<sub>2</sub>. A nanoclusters like (Bi<sub>2</sub>O<sub>3</sub>)<sub>5</sub> can react with CO<sub>2</sub> in the presence of other compounds to achieve CO<sub>2</sub> reduction.<sup>2</sup>

Various reaction pathways for CO<sub>2</sub> reduction using (Bi<sub>2</sub>O<sub>3</sub>)<sub>5</sub> were simulated in this study. It was found that bringing ethylene close enough to CO<sub>2</sub> can generate a stable intermediate, being achieved on the excited state potential energy surface. Additionally, if one Bi atom in (Bi<sub>2</sub>O<sub>3</sub>)<sub>5</sub> is replaced with Fe, the reaction can subsequently conduct at the ground state.

After testing different reaction routes, we consider that ethylene can abstract an oxygen atom out of CO<sub>2</sub> to reduce CO<sub>2</sub> to CO and generate acetaldehyde with (Bi<sub>2</sub>O<sub>3</sub>)<sub>5</sub>. Moreover, CO would generate acrolein with additional ethylene.

## References

1. P. Deng, F. Yang, Z. Wang, S. Chen, Y. Zhou, S. Zaman, B. Y. Xia, *Angew. Chem. Int. Ed.* 59, 10807–10813 (2020).
2. G. Geudtner, P. Calaminici, A. M. Köster, *J. Phys. Chem. C* 117, 13210–13216 (2013).

## **Direct growth of continuous Carbon Nitride film by thermal vapor deposition for photocatalytic applications**

Chang Shuo Yun,

Email: [andante100000@gmail.com](mailto:andante100000@gmail.com)

Phone number: 0967227476

Prof. Ly-Chong Chen\*

*National Tsing Hua University (NTHU), Chemistry Department*

*Taiwan International Graduate Program (TIGP), Molecular Science and Technology (MST) Program*

*Institute of Atomic and Molecular Sciences, Academia Sinica, Taipei 10617, Taiwan*

*Academia Sinica, Nankang, Taipei 11529, Taiwan*

CO<sub>2</sub> reduction reaction (CO<sub>2</sub>RR) has become one of the remedies for reducing carbon concentrations. Utilizing 2D semiconductor materials as catalysts has become a novel and promising method for performing catalytic reactions, whether through electro- or photocatalysis. In particular, photocatalytic reactions, so-called “Artificial Photosynthesis”, give us a sustainable method to convert CO<sub>2</sub> into fuel for further utility. Graphitic carbon nitride (g-C<sub>3</sub>N<sub>4</sub>), with its layer structure, high chemical stability, and suitable band structure, has attracted significant attention as a photocatalyst for CO<sub>2</sub> reduction reactions (CO<sub>2</sub>RR). Its moderate band gap (~2.7 eV) allows it to absorb visible light, making it a promising candidate for solar-driven CO<sub>2</sub> conversion.

# Photoelectric Interaction in Micro-LED: Correlating PL Response with Circuit Conditions

**Shih-Chieh Chen, Ting-Hua Lu**

Department of Physics, National Taiwan Normal University  
e-mail: qwe0956584768@gmail.com



## **ABSTRACT**

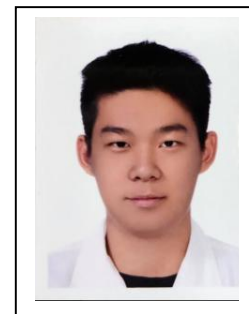
(times new roman 12pt)

The interaction between optical excitation and electrical bias in micro-light-emitting diodes (micro-LEDs) plays a crucial role in shaping carrier dynamics within quantum well structures. In this study, we investigate a GaN-based micro-LED under 360 nm laser excitation, measuring both photoluminescence (PL) spectra and photocurrent across three circuit conditions: open circuit, closed circuit without bias, and closed circuit with applied voltage. The PL spectra reveal three main emission bands—Purple Band (410 nm), Blue Band (460 nm), and Yellow Band (580 nm)—associated with band-to-band recombination, excitonic recombination, and deep-level states, respectively. Once the LED is electrically connected, even without external bias, the excitonic (Blue Band) emission disappears, and a reverse photocurrent is generated, increasing proportionally with laser power. These results suggest that photo-excited carriers are extracted by the built-in electric field instead of forming excitons. Upon application of a forward voltage, both band-to-band and excitonic emissions recover, while the deep-level emission remains largely unchanged. This study provides insight into the underlying photoelectric coupling mechanisms in micro-LEDs and highlights the influence of external circuit conditions on carrier recombination behavior.



# Electrodeposited biocompatible Fe-Mo/CP electrode catalyst for efficient CO<sub>2</sub> fixation by integrating hydrogenotrophic bacterium *Ralstonia eutropha* H16

**Chun-Wei Chou, Ming-Hsi Chiang**



Affiliation: Institute of Atomic and Molecular Science, Academia Sinica  
National Tsing Hua University  
e-mail: zcw112023457@gapp.nthu.edu.tw

## ABSTRACT

Hydrogen-driven microbial electrosynthesis (MES) represents a promising bio-electrochemical approach for converting CO<sub>2</sub> into value-added compounds. While the efficiency of microbial fermentation in MES is highly dependent on the rate of H<sub>2</sub> generation, conventional high-performance metallic H<sub>2</sub>-evolving catalysts (HECs) often produce cytotoxic byproducts, such as H<sub>2</sub>O<sub>2</sub> and metal ions, which may lead to a significant threat to microbial survival. Therefore, in this work, we evaluate cytotoxicity of different metal ions to design a biocompatible metallic hydrogen-evolving catalyst (HEC). Among them, 100mM of Mo, V, W, Ca, Al, Mg, Fe shows good biocompatibility in bacterial culture. By electrodepositing these selected metal ions onto carbon paper, the Fe-Mo/CP catalyst was fabricated and demonstrated the highest hydrogen evolution reaction (HER) activity, achieving a potential of 490 mV at 10mA cm<sup>-2</sup> in 1M potassium phosphate buffer (KPi). The Tafel slope of 120mV dec<sup>-1</sup> further indicates its favorable reaction kinetics. Moreover, under bulk electrolysis at 10mA cm<sup>-1</sup>, the Fe-Mo/CP catalyst shows negligible H<sub>2</sub>O<sub>2</sub>, indicating great potential of the catalyst applied in bio-electrochemical CO<sub>2</sub> fixation system.

# Incommensurate Charge Density Wave Order in Dirac Nodal-Line Semimetals of $\text{GdSb}_{0.7}\text{Te}_{1.3}$

**Somboon Fongchaiya<sup>1,2,3</sup>, Ming-Wen Chu<sup>3</sup> and Chao-Sung Lin<sup>1,2</sup>**

<sup>1</sup>International Graduate Program of Molecular Science and Technology (NTU-MST), National Taiwan University

<sup>2</sup>Department of Materials Science and Engineering, National Taiwan University

<sup>3</sup>Center for Condensed Matter Sciences, National Taiwan University,  
d09551007@ntu.edu.tw



## ABSTRACT

$\text{GdSb}_{0.7}\text{Te}_{1.3}$  is an orthorhombic Dirac semimetal crystal (space group  $\text{Pmmn}$ ), exhibits an incommensurate charge density wave (CDW)<sup>1</sup>. This material features a Dirac nodal line and diamond-shaped Fermi surface nesting near the Fermi level, primarily from the Sb-p orbital, along the  $\Gamma$ -X and  $\Gamma$ -M directions<sup>2</sup>. The distortion of the Sb-Sb square lattice network contributes to the formation of a one-dimensional CDW. This CDW is driven by the anisotropy of the  $p_x$  and  $p_y$  orbitals, which generates a periodic distortion pattern in real space along either the a- or b-axis. The superposition of these anisotropic orbitals can lead to a perpendicular domain structure of qa and qb domains. Using scanning transmission electron microscopy (STEM), we revealed this domain structure, which is dominated by the degeneracy of the  $p_x$  and  $p_y$  orbitals. We also visualized the incommensurate wave pattern through atomic position refinement of the Sb-sublattice in HAADF images. Furthermore, temperature-dependent experiments showed a CDW transition temperature at approximately 950 K

## References

1. S. Lei et al., **Charge Density Waves and Magnetism in Topological Semimetal Candidates  $\text{GdSb}_x\text{Te}_{2-x-\delta}$** , Adv. Quantum Technol., 1900045 (2019).
2. S. Lei et al., **Band Engineering of Dirac Semimetals Using Charge Density Waves**, Adv. Matter., 2101591 (2021).

# Texture control to achieve high in-plane thermoelectric performance in polycrystalline tin monosulfide (SnS) co-doped with silver and sodium

**M. Y. Fakhri, L. C. Chen, and K. H. Chen**

International Graduate Program of Molecular Science and Technology (NTU-MST), National Taiwan University  
Institute of Atomic and Molecular Sciences, Academia Sinica  
Centre for Condensed Matter Sciences, National Taiwan University  
e-mail: d08551006@ntu.edu.tw



## ABSTRACT

Tin monosulfide (SnS), an affordable group IV-VI compound, has emerged as a promising material due to its low toxicity, abundance, and potential for future semiconductor devices. The exceptionally low thermal conductivity from the strong lattice anharmonicity makes this material suitable for thermoelectric applications<sup>1</sup>. In general, the polycrystalline thermoelectric properties tend to show poor quality compared to its single-crystal counterpart<sup>2</sup>. Furthermore, the anisotropic performance based on the sintering process complicates the polycrystalline preparation of this material<sup>3</sup>. In this study, we successfully improved the electronic transport properties of polycrystalline SnS by utilizing the in-plane transport properties with texture modulation. It was found that the anisotropic transport properties were not only from the preferred orientation of the crystallite grain due to sintering but also from the strain of the out-of-plane SnS crystal, which led to enhanced in-plane electrical conductivity. Here, the enhancement of transport properties, by employing the lateral crystal structure, realized the highest reported electrical conductivity of polycrystalline SnS. Additionally, the hole carrier concentration of p-type SnS was further optimized by co-doping of silver and sodium. With these improvements, our co-doped SnS exhibits a relatively high power factor (PF) peak of  $\sim 4.49 \mu\text{W cm}^{-1} \text{ K}^{-2}$  at 473 K and a high thermoelectric figure of merit,  $zT$ ,  $\sim 0.3$  at 573 K, making it promising for low-temperature applications involving sulfur-based polycrystalline thermoelectric materials.

## References

1. Wu, H. et al. **Sodium-doped Tin Sulfide Single Crystal: A Nontoxic Earth - Abundant Material with High Thermoelectric Performance**. *Adv. Energy Mater.* 8, 1 – 8 (2018).
2. Zhou, B. et al. **Thermoelectric properties of SnS with Na-doping**. *ACS Appl. Mater. Interfaces* 9, 34033–34041 (2017).
3. Asfandiyar et al. **Thermoelectric SnS and SnS-SnSe solid solutions prepared by mechanical alloying and spark plasma sintering: Anisotropic thermoelectric properties**. *Sci. Rep.* 7, 1–7 (2017).

# Temperature-Dependent Valley Polarization of MoS<sub>2</sub>/Graphene Heterostructure by Resonant Polarization-Resolved PL Spectroscopy

**Yu-Chiao Chan<sup>a\*</sup>, Yu-Chen Chang<sup>a</sup>, and Ting-Hua Lu<sup>a</sup>**

<sup>a</sup>Department of Physics, National Taiwan Normal University, Taipei, Taiwan

\*chiao910727@gmail.com



## ABSTRACT

Monolayer molybdenum disulfide (MoS<sub>2</sub>) is a transition metal dichalcogenide with two-dimensional layered structure which has high potential for a wide range of applications, especially in the field of "Valleytronics". Its intrinsic valley degeneracy enables electrons to move freely between different valleys, providing additional degree of valley freedom and making it an ideal candidate for studying electron spin and valley polarization phenomena. In this experiment, we transferred hexagonal boron nitride, graphene, and molybdenum disulfide onto a silicon substrate. We investigated the phenomenon of valley polarization in monolayer molybdenum disulfide by exciting it with circularly polarized light at a wavelength of 633 nm, which is close to its band gap. From the polarized photoluminescence spectra of MoS<sub>2</sub> under different heterostructures, we observed that the degree of valley polarization is significantly enhanced when MoS<sub>2</sub> is stacked with graphene. To quantify the degree of polarization, we used the following formula:

$$DoCP(\%) = \frac{I_{\sigma+} - I_{\sigma-}}{I_{\sigma+} + I_{\sigma-}} \times 100\%$$

where  $I_{\sigma+}$  and  $I_{\sigma-}$  represent the intensities of right-hand and left-hand circularly polarized scattered light, respectively. In addition, the experimental results showed that as the temperature decreases, both the photoluminescence intensity and the degree of polarization increased significantly, confirming the enhancement of the valley polarization phenomenon at low temperatures. In summary, the distinctive valley and spin characteristics of MoS<sub>2</sub>, combined with the ability to control these properties optically at different temperatures, provide important experimental support and a theoretical foundation for valleytronics research and applications. In the future, deeper analyses will focus on stacking different materials to further explore their optical properties under diverse environmental conditions. This exploration aims to advance the design of new electronic devices and optical materials.

## References

1. A. T. Hanbicki, G. Kioseoglou, M. Currie, C. S. Hellberg, K. M. McCreary, A. L. Friedman, and B. T. Jonker, *Scientific Reports* 6, 18885 (2016).
2. S. Golovynskyi, I. Irfan, M. Bosi, L. Seravalli, O. I. Datsenko, I. Golovynska, B. Li, D. Lin, J. Qu, *Applied Surface Science* 515, 146033 (2020).



# Chemical Modulation of Magnetic Phase Transitions in One-Dimensional Covalent Organic Frameworks

**Ying-Xin Li<sup>1</sup>, Dong-Rong Wu<sup>1,2</sup>, Hsin-Ya Tsai<sup>1</sup>, Jung-Yin, Hsiao<sup>1</sup>, Elise Y.T. Li<sup>\*1</sup>**

<sup>1</sup> Department of Chemistry, National Taiwan Normal University, Taipei, Taiwan

<sup>2</sup> Department of Chemistry, University of Wisconsin–Madison, Madison, WI, USA

Speaker's email: 61242105s@gapps.ntnu.edu.tw

## ABSTRACT

Traditionally focusing on metal alloys and oxides, spintronics aims to control materials' spin states and magnetic phase transitions. Non-metallic systems, particularly organic and low-dimensional materials, are attracting more attention in recent years. Low-dimensional graphene-based materials (LGMs) exhibit diverse magnetic phases due to sublattice imbalances and topological edge states, which can be tuned by edge or junction structure engineering. Building on this concept, we designed one-dimensional covalent organic frameworks (1D-COFs) composed of triangular phenalenyl units linked via CH<sub>2</sub>, COH, or NH groups to achieve tunable spin ordering. Tight-binding and density functional theory calculations reveal that the magnetic phases of these 1D-COFs follow Lieb's theorem and can be chemically modulated. This work demonstrates a promising strategy to realize controllable magnetic transitions in organic frameworks, potentially enabling low-cost, energy-efficient, high-speed spintronic devices.

## References

1. Hirohata, A. et al. **Future perspectives for spintronic devices**, 47, 193001(2014)
2. Li, X.; Yang, J. **First-principles design of spintronics materials**, 3, 365–381(2016)
3. Zhang, L. et al. **Recent progress and challenges in magnetic tunnel junctions with 2D materials for spintronic applications**, 8, 021308(2021)

Corresponding Author: Elise Y.T. Li

Tel: + 886-2-7749-6218, Fax: + 886-2-7749-6218,

E-mail: eliseytl@ntnu.edu.tw

# Tailoring C<sub>3</sub>N<sub>4</sub> Nanotubes with Metals for Efficient CO Electroreduction to C<sub>1</sub>/C<sub>2</sub> Products

**Hung-Hsi Tsai<sup>1</sup>, Chi-You Liu<sup>\*1,2</sup>, Elise Yu-Tzu Li<sup>\*1</sup>**

<sup>1</sup>*Department of Chemistry, National Taiwan Normal University, Taipei, Taiwan*

<sup>2</sup>*Department of Chemistry, Soochow University, Taipei, Taiwan*  
*e-mail: eliseytlei@ntnu.edu.tw*



## ABSTRACT

The electrochemical CO<sub>2</sub> reduction reaction (CO<sub>2</sub>RR) is a promising approach to CO<sub>2</sub> conversion. As a downstream process after CO<sub>2</sub>RR, the CO reduction reaction plays a crucial role in extending the reaction pathway to produce C<sub>1</sub> and C<sub>2+</sub> products. Our previous results have shown that the CO<sub>2</sub> can be reduced to CO on Fe or Cu decorated C<sub>3</sub>N<sub>4</sub> nanotubes (CNNTs) with high selectivity. In this study, we consider the further conversion of CO to C<sub>1</sub> or C<sub>2</sub> products on these types of materials. The free energy diagram as well as the overpotentials of each reaction pathway are calculated, and the electronic structures of the catalysts are also analyzed. Based on our results, we evaluate the potential of CO conversion catalysts and provide a basis for the design of advanced energy materials.

## References

1. Gracia, J.; Kroll, P. **First principles Study on C<sub>3</sub>N<sub>4</sub> Carbon Nitride Nanotubes.** *J. Mater. Chem.* **19**, 3020-3026- (2009).
2. Liu, C. Y.; Li, E. Y. **Intrinsically Functionalized Fe/C<sub>3</sub>N<sub>4</sub> Nanotubes Display PH-Dependent Oxygen Reduction Overpotentials.** *ACS Appl. Energy Mater.* **7**, 2416-2422- (2024)
3. Liu, C. Y.; Li, E. Y. **High Selectivity in CO<sub>2</sub> Reduction to CO Using Metal-Decorated C<sub>3</sub>N<sub>4</sub> Nanotubes.** *ACS Appl. Energy Mater.* **7**, 8155-8162- (2024)

# Strain-Modulated Electrocatalytic Activity of Fe-Decorated g-C<sub>3</sub>N<sub>4</sub> Surfaces

**Sih-Ling Hsu<sup>1</sup>, Chi-You Liu<sup>\*1,2</sup>, Elise Y. Li<sup>\*1</sup>**

<sup>1</sup> Department of Chemistry, National Taiwan Normal University, Taipei, Taiwan

<sup>2</sup> Department of Chemistry, Soochow University, Taipei, Taiwan

e-mail: eliseyli@ntnu.edu.tw / cy.liu@scu.edu.tw

## ABSTRACT

Strain engineering has emerged as a promising approach to modulate the activity of catalysts, particularly in the two-dimensional materials. The MN<sub>x</sub> active centers on carbon-based materials offer high activity and tunable electronic properties for catalytic reactions as a conventional single atom catalyst (SAC). Here, we simulate the Fe-decorated C<sub>3</sub>N<sub>4</sub> surfaces at different compressive strains, and demonstrate how strain affects the electronic structure, molecular adsorption energies, and overall oxygen reduction reaction (ORR) performance. Our investigations from the microscopic perspective provides design principles of high performance electrocatalysts for fuel cells, metal-air batteries, and other renewable energy technologies.

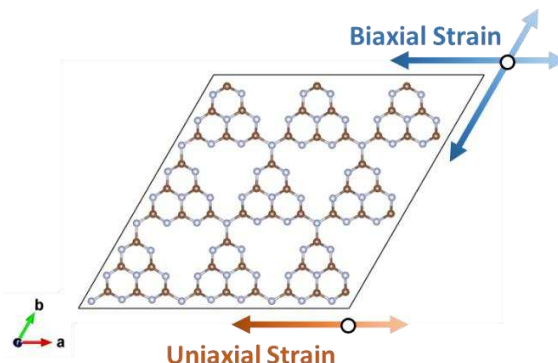


**Figure.** Schematic representations of the applied biaxial and uniaxial strain on g-C<sub>3</sub>N<sub>4</sub>.

## References

1. J. Kim, S. Kim, E. Jung, D. H. Mok, V. K. Paidi, J. Lee, H. S. Lee, Y. Jeoun, W. Ko, H. Shin, B. Lee, S. Kim, H. Kim, J. H. Kim, S. Cho, K. Lee, S. Back, S. Yu, Y. Sung, T. Hyeon **Adv. Funct. Mater.**, 32, 2110857 (2022).
2. H. Niu, X. Wang, C. Shao, Y. Liu, Z. Zhang, Y. Guo **J. Mater. Chem. A**, 8, 6555-6563 (2020).
3. J. Su, C. B. Musgrave, Y. Song, L. Huang, Y. Liu, G. Li, Y. Xin, P. Xiong, M. M.-J Li, H. Wu, M. Zhu, H. M. Chen, J. Zhang, H. Shen, B. Z. Tang, M. Robert, W. A. Goddard, R. Ye **Nat. Catal.**, 6, 818-828 (2023).

# Edge Morphology Control on the Topological Structures and Magnetic Properties of Chiral Graphene Nanoribbons

**Zi-Xuan Tang, Jung-Yin Hsiao and Elise Yu-Tzu Li\***

Department of Chemistry, National Taiwan Normal University, Taipei 116-059, Taiwan  
61242057s@gapps.ntnu.edu.tw

## ABSTRACT

Graphene nanoribbons (GNRs) are one-dimensional materials with potential applications on electronic device components<sup>[1]</sup>. In this study, the topological properties of finite carbon nanotubes (CNTs) with specific terminal geometries are expanded and generalized to chiral graphene nanoribbons, focusing on the magnetic interactions of topological graphene edge states<sup>[2]</sup>. Validating this applicability is critical for advancing the theoretical

framework and design principles of carbon-based nanostructures. Density functional theory (DFT) calculations were conducted using Quantum ESPRESSO, including band structure and spin polarization analyses to evaluate the electronic structure and magnetization. In particular, the magnetism of GNRs can be controlled and modulated by boundary carbon modification via selective hydrogenation<sup>[3]</sup>. We applied four specific modification rules to the terminal carbons, systematically examining symmetric and asymmetric edge structures (see Figure 1a). Ferromagnetic or antiferromagnetic behaviors can be predicted and regulated by combinations of modification patterns. The magnitude of the edge magnetic moment exhibits mathematical relationships with the chirality as well as the edge morphology type (see Figure 1b). These findings validate the applicability of CNT-derived formulas to GNRs, suggesting broader relevance to other carbon-based nanostructures and their potential for practical applications. These results contribute to the material design principles of spintronic applications of chiral GNRs.

[1-3]

## References

- [1] V. Saraswat, R. M. Jacobberger, M. S. Arnold, *ACS nano* **2021**, *15*, 3674–3708.
- [2] J.-Y. Hsiao, C.-Y. Liu, E. Y. Li, *Journal of Materials Chemistry C* **2023**, *11*, 15001–15007.
- [3] S. Song, Y. Teng, W. Tang, Z. Xu, Y. He, J. Ruan, T. Kojima, W. Hu, F. J. Giessibl, H. Sakaguchi, *Nature* **2025**, 1–7.

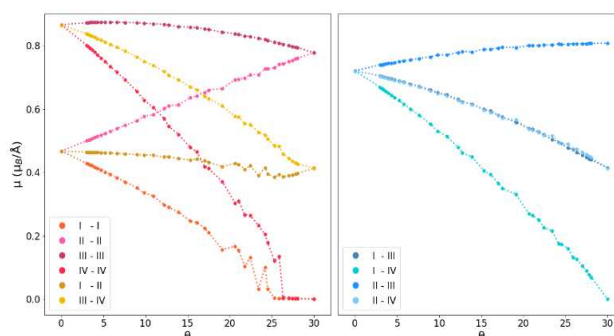


Fig. 1 The relationship between magnetization  $\mu$  (in  $\mu_B/\text{\AA}$ ) and chirality  $\theta$  (in  $^\circ$ ) for ten edge mode combinations derived from four modes on two edges.



# Peptide-based AIE fluorescent tag for detecting the amyloid formation by islet amyloid polypeptide

**Shu-An Shih, Ling-Hsien Tu\***

Department of Chemistry, National Taiwan Normal University, Taipei, Taiwan  
e-mail: shuannshi@gmail.com

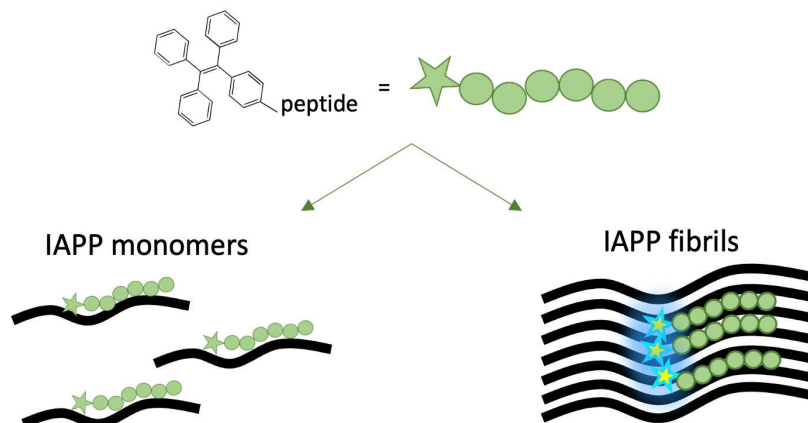


## ABSTRACT

Islet amyloid polypeptide (IAPP), or amylin, is a 37-residue peptide hormone that is co-expressed and co-secreted with insulin by pancreatic  $\beta$ -cells. In its monomeric state, IAPP is classified as an intrinsically disordered protein. Nonetheless, accumulating evidence implicates its aggregation into oligomers and cross- $\beta$  sheet amyloid fibrils in the dysfunction and apoptosis of  $\beta$ -cells. This aggregation is a pathological hallmark of type 2 diabetes mellitus, marked by amyloid deposition in the islets of Langerhans.

Conventional bioprobes, including Thioflavin T and Congo red, have been employed to detect IAPP aggregation. However, their utility is hampered by the aggregation-caused quenching (ACQ) effect. Fluorophores with aggregation-induced emission (AIE) characteristics offer a solution to this limitation, providing low background fluorescence, high sensitivity, and improved signal-to-noise ratios.

In this work, we present and continuously optimize peptide-based AIE probes designed to monitor the aggregation of fibrillogenic IAPP. These probes combine an AIE fluorophore with a peptide sequence that exhibits strong binding affinity to IAPP. Upon interaction with IAPP aggregates, restricted intramolecular motions trigger fluorescence activation, while probes remain non-emissive in aqueous environments or when bound to monomeric IAPP. This fluorescence switching mechanism enables reliable differentiation between monomeric and aggregated IAPP, providing a powerful tool for studying IAPP aggregation dynamics and their role in the pathogenesis of diabetes.



# Enhancing Equivariant Flow Matching for 3D Structure Generation with the Extended Features

**Cheng-Wei Tsai, and Ming-Kang Tsai**

*Department of Chemistry and Intelligent Computing for Sustainable Development Research Center, National Taiwan Normal University, Taipei 11677, Taiwan*  
e-mail: tomas890812@gmail.com



## ABSTRACT

Generating accurate 3D molecular structures is one of the fundamental tasks in computational chemistry, and it provides critical implications for the application of drug discovery, materials design, and molecular property prediction. For the molecular generative artificial intelligence, the equivariant diffusion models (EDMs) have demonstrated strong performance by leveraging symmetry-preserving neural architectures. However, these models often suffer from unstable probabilistic dynamics and inefficient sampling. In this work, we explore EquiFM<sup>1</sup>, a generative model based on similar equivariant principles, which jointly predicts categorical (atom types) and continuous (atomic coordinates) features for 3D molecular generation. In this study, our ML exercises using QM9 dataset reveal that EquiFM does not significantly outperform EDM in key evaluation metrics, including molecular validity, stability, and property prediction accuracy. To address this, we plan to introduce two additional structure-aware features: interatomic distances derived from Cartesian coordinates and bond step features<sup>2</sup> capturing molecular connectivity patterns. These features are naturally compatible with the equivariant design of EquiFM and provide rich geometric and topological information. We attempt to incorporate these features to potentially improves the performance of EquiFM across multiple molecular generation benchmarks, offering enhanced validity, diversity, and property distribution alignment in the generated molecules.

## References

1. Y. Song, J. Gong, M. Xu, Z. Cao, Y. Lan, S. Ermon, H. Zhou, W.-Y. Ma, **Equivariant Flow Matching with Hybrid Probability Transport for 3D Molecule Generation**, *OpenReview*. (2023)  
<https://openreview.net/forum?id=hHUZ5V9XFu>
2. Z.-R. Ye, S.-H. Hung, B. Chen, and M.-K. Tsai, **Assessment of predicting frontier orbital energies for small organic molecules using Knowledge-Based and Structural Information**, *ACS Engineering Au*, vol. 2, no. 4, pp. 360–368, (2022), doi: 10.1021/acsengineeringau.2c00011.

# Investigating Soluble Protein Tags for Calcitonin Aggregation Inhibition

Po-Chun Cheng, Ling-Hsien Tu

Department of Chemistry, National Taiwan Normal University, Taipei  
11677, Taiwan  
e-mail: [jasonpochung@gmail.com](mailto:jasonpochung@gmail.com)



## ABSTRACT

Human calcitonin (hCT) is a 32-amino-acid peptide hormone secreted by the parafollicular cells (C cells) of the thyroid. Its primary physiological function is to lower blood calcium levels and regulate phosphate concentration in the bloodstream. It is also used clinically for treating bone-related diseases. However, hCT has a strong tendency to aggregate, which reduces its therapeutic efficacy. To address this issue, our lab has been developing peptides with high sequence homology to hCT using computational design and sequence prediction tools. We created a double mutant hCT (DM hCT) by substituting Leucine at position 12 and Histidine at position 17. Previous experiments showed that DM hCT exhibited a much longer lag time for aggregation than wild type hCT. Fibril formation still occurred, indicating that DM hCT's anti-aggregation effect has room for further optimization. DM hCT is considered a low-aggregation variant of hCT. It is speculated that the Histidine substitution introduces partial positive charges, thereby increasing the net charge of the peptide and reducing its tendency to form amyloid-like fibrils. To enhance the solubility and further suppress the aggregation of DM hCT, we plan to fuse a specific sequence tag at the C-terminus of DM hCT. This fusion tag approach aims to increase solubility and exert an anti-aggregation effect. Positively charged amino acids—lysine, arginine—and the hydrophilic residue asparagine are selected as components of the peptide tags. Numbers of residue repeat will be investigated to meet our aim. In addition, we designed a couple of incubation conditions to evaluate the solubility of DM hCT and these variants. Thioflavin T (ThT) binding fluorescence will be applied to monitor peptide aggregation, to evaluate the anti-aggregation effect of the designed peptide tags.

## References

1. Yi-Ting Chen, Kai-Wei Hu, Bo-Jie Huang, Chian-Hui Lai, and Ling-Hsien Tu, **J. Phys. Chem. B**, *123*, 10171–10180 (2019).
2. Mohammad Monirul Islam, Monsur A. Khan, Yutaka Kuroda, **Biochimica et Biophysica Acta**, *1824*, 1144–1150 (2012).

# Thermoresponsive Dual-Functional Gelatin Hydrogels for Inhibition of Human Calcitonin Amyloid Formation



**Yun-Hsuan Chen<sup>a</sup>, Yi-Cheun Yeh<sup>b</sup>, Ling-Hsien Tu<sup>a\*</sup>**

<sup>a</sup>Department of Chemistry, National Taiwan Normal University, Taipei  
116, Taiwan

<sup>b</sup>Institute of Polymer Science and Engineering, National Taiwan University, Taipei  
10617, Taiwan  
e-mail: w41321@gmail.com

## ABSTRACT

Human calcitonin (hCT) is a 32-amino-acid peptide hormone secreted by thyroid C-cells, and it plays an essential role in regulating blood calcium levels. However, its inherent instability and high tendency to form amyloid fibrils greatly limit its therapeutic application. To address this major shortcoming, gelatin-based hydrogels were applied in this study to improve hCT stability. Gelatin is a widely available, cost-effective natural biopolymer with excellent biocompatibility and biodegradability, which has long been used in drug delivery systems<sup>1</sup>. Nevertheless, conventional gelatin hydrogels often exhibit insufficient structural stability at physiological temperatures and lack the ability to effectively prevent peptide aggregation. Herein, a dual-functional gelatin-based hydrogel was developed. The addition of polydextran aldehyde (PDA) was expected to form reversible imine bonds with amino groups in gelatin<sup>2</sup>, thereby enhancing the hydrogel's crosslinking density and structural stability. Meanwhile, catechol moieties were grafted onto gelatin (DHCA-GelB) to impart polyphenol functionality, aiming to inhibit hCT amyloid fibril formation and maintain its biological activity. This work demonstrates that the developed gelatin/PDA/DHCA-GelB hydrogel system is thermoresponsive and possesses anti-amyloidogenic capacity, highlighting its potential as a peptide drug carrier for stabilizing hCT and preventing amyloid formation.

## References

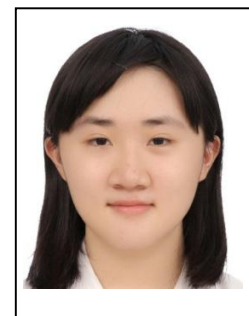
1. S. Young, M. Wong, Y. Tabata, A.G. Mikos, **Journal of Controlled Release**, *109*, 256–274 (2005).
2. X.-E. Chen, C.-J. Yan, C.-H. Lu, Y.-C. Yeh, **ACS Applied Polymer Materials**, *6*, 7340–7356 (2024).



# **Investigating azide-alkyne cycloaddition in the presence of TFE to create stabilized helical DM hCT fragment for inhibition of calcitonin amyloid**

**Yu-Hsuan Chang, and Ling-Hsien Tu**

Department of Chemistry, National Taiwan Normal University, Taipei  
116, Taiwan  
e-mail: kokichi0621@gmail.com



## **ABSTRACT**

While human calcitonin (hCT), a 32-amino-acid hormone secreted by the thyroid's parafollicular cells, is widely used for treating bone-related diseases like osteoporosis, its therapeutic potential is significantly hindered by peptide aggregation, which limits its bioavailability.<sup>1</sup> A promising strategy to combat this has been the inclusion of DM hCT 1-22 (a 1-22 fragment of Y12LN17H hCT), known to reduce fibril formation.<sup>2</sup> This fragment's effectiveness is believed to be linked to its assumed  $\alpha$ -helical structure. However, a key challenge is that DM hCT 1-22 does not readily adopt an  $\alpha$ -helical structure in aqueous solutions without the assistance of inducing agents, such as trifluoroethanol (TFE).<sup>3</sup> To enhance the inhibitory effect of DM hCT 1-22, our research introduces a novel approach: cyclizing this peptide via azide-alkyne cycloaddition in the presence of TFE.<sup>4</sup> This specific reaction condition represents an unexplored area.

Our initial steps involved synthesizing DM A1, a DM hCT 1-22-related peptide, by strategically modifying Gly-10 and Gln-14 with azidohomoalanine (Aha) and propargylglycine (Pra), respectively, introducing the necessary azide and alkyne groups for cyclization.<sup>5</sup> The subsequent experimental protocol is structured to first determine the optimal TFE concentration required to induce an  $\alpha$ -helical structure in DM A1, confirmed using circular dichroism (CD) spectrometry.<sup>6</sup> Following this, the peptide will undergo cyclization by reaction with CuSO<sub>4</sub> and sodium ascorbate within a mixture of water, tert-butanol, and TFE, with heating at 50–60°C for two hours. The final cyclized product will then be re-analyzed by CD spectrometry. Ultimately, its ability to inhibit hCT fibrillization will be thoroughly evaluated using thioflavin-T kinetic assays and transmission electron microscopy.

## **References**

1. Y.-T. Chen; K.-W. Hu; B.-J. Huang; C.-H. Lai; L.-H. Tu, **Inhibiting Human Calcitonin Fibril Formation with Its Most Relevant Aggregation-Resistant Analog**, *J. Phys. Chem. B*, 123, 10171–10180- (2019).
2. Y.-P. Chuang ; Y.-P. Chang ; L.-H. Tu, **Investigating the Inhibitory Property of DMhCT on hCT Fibrillization via Its Relevant Peptide Fragments**, *Protein Science*, 32, e4711-(2023).
3. J. Vymet'ál; L. Bednářová; J. Vondrašek, **Effect of TFE on the Helical Content of AK17 and HAL-1 Peptides: Theoretical Insights into the Mechanism of Helix Stabilization**, *J. Phys. Chem. B*, 120, 1048–1059-(2016).

4. Y. H. Lau ; P. de Andrade ; Y. Wu ; D. R. Spring, **Peptide Stapling Techniques based on Different Macrocyclization Chemistries**, *Chem. Soc. Rev.*, *44*, 91-102 (2015).
5. C. N. Pace ; J. M. Scholtz, **A Helix Propensity Scale Based on Experimental Studies of Peptides and Proteins**, *Biophysical Journal*, *75*, 422–427 -(1998).
6. A. Motta ; G. Strazzullo ; M.A. Castiglione Morelli, **Conformational Flexibility in Calcitonin the Dynamic Properties of Human and Salmon Calcitonin in Solution**, *J Biomol MR*, *13*(2) 161-74-(1999).

# Rational Design of hIAPP Variants with Potent Antibacterial Activity through Targeted Arginine Substitutions.

**Wei-Fan Hsu, Pei-Ya Shan, and Ling-Hsien Tu**

Department of Chemistry, National Taiwan Normal University, Taipei  
116, Taiwan  
e-mail: 41142103S@gapps.ntnu.edu.tw



## ABSTRACT

Human islet amyloid polypeptide (hIAPP) has recently been reported to exhibit antibacterial activity, highlighting its potential as a therapeutic agent to reduce reliance on traditional antibiotics, which are often associated with drug resistance. Enhancing the antibacterial activity of hIAPP may therefore provide a novel approach to combating antimicrobial resistance.

Previous studies<sup>1,2</sup> have suggested that the cytotoxic properties of hIAPP are closely related to its structural and functional similarity with the antimicrobial peptides (AMPs), as both could interact with and disrupt bacterial membranes. Additionally, introducing positively charged amino acid substitutions at aggregation-prone regions of amyloid peptides has been shown to improve antimicrobial activity<sup>3</sup>, implying this strategy may also be effective for hIAPP.

Earlier research<sup>4</sup> examined G33K and G24K hIAPP mutants and found improvement in antibacterial activity. Building upon this, the present study aims to explore additional substitution sites and amino acids to develop hIAPP variants with enhanced antimicrobial properties.

In this study, positively charged amino acid substitutions were introduced into hIAPP to enhance antibacterial activity. Variants including G24R-IAPP and F23R-IAPP were chosen by the FoldAmyloid prediction tool. Our workflow involved synthesizing peptides with an automated microwave peptide synthesizer and purifying them through high-performance liquid chromatograph. We then used MALDI-TOF mass spectrometry to determine their precise monoisotopic masses. For functional characterization, we assessed aggregation behavior using a Thioflavin T kinetic assay, determined secondary structure via circular dichroism, and measured antibacterial activity with both broth and agar dilution methods.

## References

1. L. Khemtémourian, J.A. Killian, J.W. Höppener, M.F. Engel, **Experimental Diabetes Research**, 2008, 421287 (2008).
2. V. Baltutis, P. D. O'Leary, L. L. Martin, **ChemPlusChem**, 87, e202200240 (2022).
3. M. Torrent, J. Valle, M. V. Nogués, E. Boix, D. Andreu, **Angew Chem Int Ed Engl.**, 50, 10686–10689 (2011).
4. P.-Y. Shan, master thesis, National Taiwan Normal University (2023).

# A Computational Study on CO<sub>2</sub> Carboxylation of Aromatic and Aliphatic Terminal Alkynes Catalyzed by Lanthanide Amide Complexes

**Yu-Rong Chen, Kai-Lin Chang, Ming-Kang Tsai**

Department of Chemistry, National Taiwan Normal University, Taipei, Taiwan

e-mail: 61342047s@gapps.ntnu.edu.tw



## ABSTRACT

In the Calvin cycle of photosynthesis, plants use ribulose-1,5-bisphosphate carboxylase/oxygenase (RuBisCO) to catalyze the reaction between ribulose-1,5-bisphosphate (RuBP) and CO<sub>2</sub>, forming two molecules of 3-phosphoglycerate (3PGA), which eventually lead to glucose synthesis.<sup>[1]</sup> This natural carbon fixation mechanism has inspired the design of catalytic systems that can efficiently convert CO<sub>2</sub> into valuable compounds. A novel bis(amidate) rare-earth metal amides, {LRE[N(SiMe<sub>3</sub>)<sub>2</sub>]·THF}<sub>2</sub> (RE = Y, La, Nd), exhibits excellent catalytic activity for the carboxylation of terminal alkynes bearing various functional groups with CO<sub>2</sub> under ambient pressure, affording high product yields. Among them, the Nd-based catalyst demonstrated the highest reactivity toward aromatic alkynes, efficiently producing various aryl-substituted propiolic acids under mild conditions. However, this catalytic system showed no reactivity toward aliphatic alkynes under the same conditions, failing to yield the desired products.<sup>[2]</sup>

To investigate the origin of this selectivity, we employed DFTB (Density Functional Tight Binding) calculations and molecular simulations to analyze the reaction pathways between different terminal alkynes (aromatic and aliphatic) and CO<sub>2</sub> within this catalytic system. By comparing transition state energy barriers and overall reaction energy profiles, we aim to elucidate the molecular basis of the observed catalytic selectivity and provide theoretical insights for improving catalytic efficiency.

## References

- [1] Tommasi, I. C. The Mechanism of Rubisco Catalyzed Carboxylation Reaction: Chemical Aspects Involving Acid-Base Chemistry and Functioning of the Molecular Machine. *Catalysts* 2021, 11, 813.
- [2] Cheng, H.; Zhao, B.; Yao, Y.; Lu, C. *Green Chem.* 2015, 17, 1675 —1682

# Computational Investigation of the Regioselective $\gamma$ -Insertion of Alkynyl Carbenes into O-H Bonds: Mechanistic Insights and Selectivity Control.

**Yumnam Nganthoinganbi,<sup>1,2</sup> Himani Vaid,<sup>3</sup> and Ming-Kang Tsai<sup>1,2\*</sup>, Ramani Gurubrahamam<sup>3\*</sup>**



<sup>1</sup> Department of Chemistry, National Taiwan Normal University, Taipei, Taiwan;

<sup>2</sup> Intelligent Computing for Sustainable Development Research Center, National Taiwan Normal University, Taipei, Taiwan;

<sup>3</sup> Department of Chemistry, Indian Institute of Technology Jammu, Jammu & Kashmir, India

Corresponding email: [guru.ramani@iitjammu.ac.in](mailto:guru.ramani@iitjammu.ac.in) and [mktsai@ntnu.edu.tw](mailto:mktsai@ntnu.edu.tw)

## ABSTRACT

This study investigates the high regioselectivity of alkynyl carbene insertion into O-H bonds, utilizing DFT calculations <sup>1</sup> for geometry optimizations and frequency analyses using the  $\omega$ B97X-D/6-31+G(d,p) method, and single-point energy corrections at the B2PLYP/6-31+G(d,p) method to enhance accuracy. Solvent effects were modeled using the SMD solvation model in DCM. Computational results reveal that using TFE as a substrate leads to both  $\gamma$ - and  $\alpha$ -products form, with  $\gamma$  being the major product. The high selectivity with TFE is attributed to its strong H-bonding ability and electronic effects, which stabilize key transition states and lower the activation energy barrier for  $\gamma$ -product formation. This selectivity follows the Curtin-Hammett principle <sup>2</sup>, where the product distribution is governed by the activation energy barriers. In addition, when using ethanol as the substrate leads solely to the  $\alpha$ -product, highlighting the role of substituent electronic effects in determining selectivity.

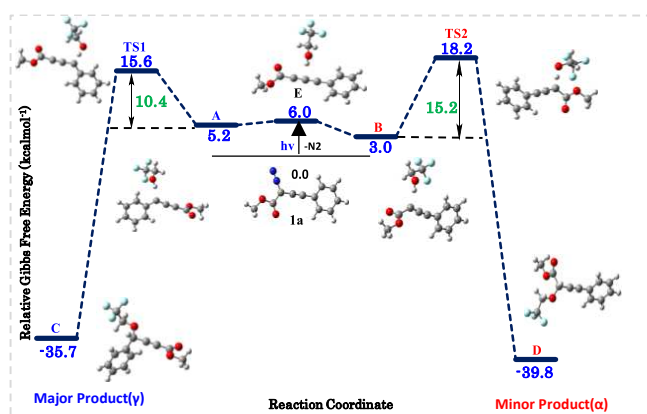


Fig: Energy Diagram for  $\gamma$ - vs.  $\alpha$ -Selective O-H Insertion.

## References

1. S. E. Wheeler, T. J. Seguin, *Acc. Chem. Res.*, **49**, 1061-1069 (2016).
2. P. S. Filby, S. Rayat, *J. Org. Chem.*, **83**, 1790-1796 (2018).



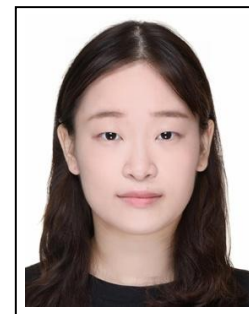
# Bismuth-Based Metal-Organic Framework with Oxidoreductase-Like Activity for Hexavalent Chromium Detection

**Yi-Ning Wang<sup>1</sup>, Sivasankar kulandaivel<sup>1</sup>, Hsin-Tsung Chen<sup>2</sup>, Yi-Chun Yeh<sup>1,\*</sup>**

<sup>1</sup>*Department of Chemistry, National Taiwan Normal University, Taipei, Taiwan 11677*

<sup>2</sup>*Department of Chemistry, Chung Yuan Christian University, Chungli District, Taoyuan City 320314, Taiwan.*

e-mail: elaine910113@gmail.com



## ABSTRACT

In this study, we present SU-101, a bismuth-based metal-organic framework (MOF) synthesized at room temperature using green solvents and plant-derived ellagic acid,<sup>[1]</sup> as a novel oxidoreductase-mimicking nanozyme for the selective colorimetric detection of hexavalent chromium (Cr<sup>6+</sup>). Unlike conventional peroxidase-like nanozymes, SU-101 catalyzes a Cr<sup>6+</sup>-driven redox reaction with 3,3',5,5'-tetramethylbenzidine (TMB) in the absence of H<sub>2</sub>O<sub>2</sub>, producing a blue-green chromogenic product detectable via UV–Vis spectroscopy. Kinetic studies reveal a low Michaelis–Menten constant ( $K_m = 0.182$  mM) for Cr<sup>6+</sup>, indicating strong substrate affinity and superior performance over H<sub>2</sub>O<sub>2</sub> ( $K_m = 212$  mM). The system achieves a low detection limit of 0.36  $\mu$ M and exhibits excellent selectivity toward Cr<sup>6+</sup> against 22 potential interfering ions. We propose a redox-mediated mechanism wherein TMB is oxidized to its colored form (TMB<sub>ox</sub>), releasing electrons that are transferred by the Bi<sup>3+</sup> clusters within SU-101. These clusters undergo a transient reduction to Bi<sup>2+</sup>, which rapidly reoxidizes to Bi<sup>3+</sup> while transferring electrons to Cr<sup>6+</sup>, thereby reducing it to Cr<sup>3+</sup>. This redox cascade underscores the unique role of Bi as an efficient electron mediator. Additionally, the reaction is inhibited by cysteine (Cys), enabling dual-analyte detection. This work introduces SU-101 as a green, biocompatible, and multifunctional platform for environmental monitoring, highlighting the untapped potential of bismuth-based MOFs in advanced sensing technologies.

## References

1. Svensson Grape, E.; Flores, J. G.; Hidalgo, T.; Martínez-Ahumada, E.; Gutiérrez-Alejandre, A.; Hautier, A.; Williams, D. R.; O’Keeffe, M.; Öhrström, L.; Willhammar, T.; Horcajada, P.; Ibarra, I. A.; Inge, A. K. **J. Am. Chem. Soc.**, 142 (39), 16795–16804 (2020).

# Photoluminescence and Raman characterization of monolayer MoS<sub>2</sub> under twisted and circularly polarized light

**Yi – Fan CHIU**

Department of Physics, National Taiwan Normal University, Taiwan  
e-mail: evan.chiou.tw@gmail.com



## ABSTRACT

This study explores the photoluminescence (PL) and Raman spectral characteristics of monolayer molybdenum disulfide (MoS<sub>2</sub>) under various excitation conditions. Using 532 nm and 633 nm laser sources, we measured PL and Raman spectra to analyze PL peak position, full width at half maximum (FWHM), intensity variation, and spectral shifts (redshift or blueshift). Characteristic Raman modes, including A<sub>1g</sub>, E<sub>2g</sub>, 2LA, c-mode, and b-mode, were recorded to investigate how excitation wavelength influences phonon behavior.

A spatial light modulator (SLM) was employed to generate laser beams carrying orbital angular momentum (OAM) with topological charges  $\ell = 0$  to 5, allowing us to study how twisted light affects the optical responses of MoS<sub>2</sub>. To minimize thermal effects from increasing beam size at higher OAM orders, measurements were conducted under low power density.

Additionally, the study incorporated circularly polarized light to introduce spin angular momentum (SAM), combining it with OAM to analyze the degree of circular polarization (DoCP) in PL under left-handed circular excitation. This approach probes helicity preservation or exchange in MoS<sub>2</sub>. Comparative measurements were also performed on MoS<sub>2</sub> deposited on sputtered platinum substrates (Pt / MoS<sub>2</sub>), evaluating their effects on PL intensity, spectral shift, and DoCP behavior. The findings contribute to a deeper understanding of light–matter interactions in two-dimensional materials and provide experimental insight for the development of spin–orbit coupled photonic devices.

## References

1. Chang, Y. C., Chan, Y. C., Das, B., Syue, J. F., Hu, H. C., Lan, Y. W., & Lu, T. H. Distinctive characteristics of exciton-phonon interactions in optically driven MoS<sub>2</sub>. *Physical Review Materials*, 8(7), 074003. (2024).
2. Mak, K. F., He, K., Shan, J., & Heinz, T. F. Control of valley polarization in monolayer MoS<sub>2</sub> by optical helicity. *Nature nanotechnology*, 7(8), 494-498. (2012).
3. Zeng, H., Dai, J., Yao, W., Xiao, D., & Cui, X. Valley polarization in MoS<sub>2</sub> monolayers by optical pumping. *Nature nanotechnology*, 7(8), 490-493. (2012)

# Chemical Vapor Deposition Synthesis of 3R-stacked Molybdenum Disulfide for ferroelectric tunnel junction transistors

**Ju-Yi Huang<sup>1</sup>, Tzu-Hao Kuo<sup>1</sup>, Min-Jia Zhang<sup>1</sup>, Shao-Yu Chen<sup>2</sup>, Yann-Wen Lan<sup>1\*</sup>**

<sup>1</sup>*Department of Physics, National Taiwan Normal University, Taipei, Taiwan*

<sup>2</sup>*Center for Condensed Matter Sciences, National Taiwan University, Taipei, Taiwan*

e-mail: ianjywork@gmail.com



## ABSTRACT

Bilayer MoS<sub>2</sub> with rhombohedral (3R) stacking lacks inversion symmetry and exhibits interlayer sliding ferroelectricity, making it a strong candidate for non-volatile memory applications. We synthesized bilayer 3R-MoS<sub>2</sub> on SiO<sub>2</sub>/Si substrates using a two-stage chemical vapor deposition (CVD) process. The resulting fan-shaped domains offer abundant sliding interfaces suitable for ferroelectric switching.

Material characterization via Raman spectroscopy and atomic force microscopy (AFM) confirmed bilayer thickness and 3R stacking, with the breathing mode appearing near 37.4 cm<sup>-1</sup>. The MoS<sub>2</sub> flakes were used to fabricate vertical ferroelectric tunnel junctions (FTJs) featuring graphene electrodes and a thin hBN dielectric layer. Fabrication steps included wet transfer, Al<sub>2</sub>O<sub>3</sub> encapsulation, and plasma etching.

Electrical measurements revealed clear bistable I–V behavior in 3R-MoS<sub>2</sub> FTJs, indicating polarization-driven switching. Control devices made from monolayer MoS<sub>2</sub> or hBN showed no such response, confirming the role of 3R ferroelectricity.

These results demonstrate the feasibility of sliding ferroelectricity in 2D systems and highlight 3R-MoS<sub>2</sub> as a promising material for low-power, scalable memory devices. Future work will focus on PUND and PFM characterization, as well as endurance testing.

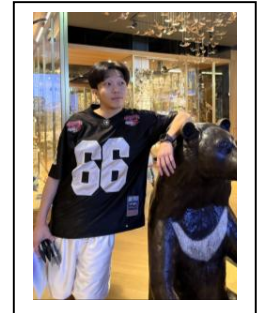
## References

- [1]. Wang, K., Xu, R., & Gao, F. et al. Controlled Epitaxial Growth of Strain-Induced Large-Area Bilayer MoS<sub>2</sub> by Chemical Vapor Deposition Based on Two-Stage Strategy. *Materials Today Physics* 46, 101501 (2024).
- [2]. Sam, R. T., Umakoshi, T., & Verma, prabhat. Probing Stacking Configurations in a Few Layered MoS<sub>2</sub> by Low Frequency Raman Spectroscopy. *Scientific reports* 10, 21227 (2020).

# Magnetic Field Driven Domain Evolution in van der Waal Material $\text{Fe}_3\text{GaTe}_2$

**Shao-Quan Chang**

Department of Physics, National Taiwan Normal University e-mail:  
jmk08957@gmail.com



## ABSTRACT

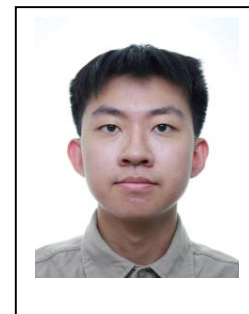
Microscopic spin-textures in two-dimensional (2D) van der Waals (vdW) ferromagnets hold great promise for next-generation spintronic devices due to their potential for high data density and low energy consumption. Among these materials,  $\text{Fe}_3\text{GaTe}_2$  (FGT) stands out for its high Curie temperature above room temperature and stable perpendicular magnetic anisotropy (PMA). Effective control of magnetic properties in vdW ferromagnets is crucial for realizing practical spintronic applications. In this work, a series of stripes and bubble domain evolution within FGT have been recorded by Kerr microscopy under external out-of-plane (OOP) magnetic field. In thin and thick FGT samples, magnetic domains undergo a transition from stripe to bubble and complex configurations, respectively, during field cooling (FC). In stripe domain configuration, we observe two distinct flip modes as the OOP magnetic field increase to saturation state and returns to the remanence state. In bubble domain configuration, hexagonal ordering of magnetic bubbles can be achieved via field-induced splitting and shaping mechanisms. Furthermore, domain elimination and merging phenomena are observed under applied in plane magnetic field. These findings offer critical insights into the field-tunable magnetic behavior of FGT and highlight its potential in spintronic applications, particularly with respect to domain manipulation and spin transport properties.

## References

1. (times new roman 12pt) F. Last name, F. Last name,... **Journal Title**, *Journal Volume Number*, Page- (YEAR).

**Graphene-Protected Interfaces in Chiral  
Perovskite/Cobalt Hetero-structures**  
**Cheng-Ying Hsiao, Po-Hsiang Hsu, Lan-Sheng  
Yang, Yan-Ru Chu, Yu-Chiang Chao, Wen-Chin  
Lin\***

Department of Physics, National Taiwan Normal University  
e-mail: wclin@ntnu.edu.tw



## ABSTRACT

Chiral perovskites are structures containing handedness (chirality), classified as dextrorotatory (right-handed) or levorotatory (left-handed). This chirality can influence their magnetic characteristics. Furthermore, using different materials allows us to control spin selectivity. In previous experiments, we coated chiral perovskites with the ferromagnetic material cobalt. The spin selectivity inherent in the chiral perovskite can interact with the magnetic material interface, enabling tunable devices. However, we observed that after coating the chiral perovskite, the cobalt saturation magnetization intensity decreased. We hypothesized that lead ions reacted with cobalt in a redox reaction. Therefore, in this experiment, we inserted graphene as an interlayer. The graphene effectively suppressed the reaction between the chiral perovskite and cobalt. Moreover, it acts as a protective layer that isolates the chiral perovskite and cobalt while still allowing us to observe their interaction. After adding the graphene protective layer, the decrease in saturation magnetization intensity became smaller, while the coercive field remained unchanged. This indicates that graphene effectively reduced the reaction between the two materials, functioning as a protective layer.

## References

1. H. Lu, J. Wang, C. Xiao, X. Pan, X. Chen, R. Brunecky, J. J. Berry, K. Zhu, M. C. Beard and Z. V. Vardeny, Science advances 5 (12), eaay0571 (2019).
2. Z. Huang, B. P. Bloom, X. Ni, Z. N. Georgieva, M. Marciesky, E. Vetter, F. Liu, D. H. Waldeck and D. Sun, ACS nano 14 (8), 10370-10375 (2020).
3. S.-Y. Liu, T.-H. Chen, B.-T. Wu, P.-H. Hsu, Z.-E. Lin, W.-H. Wang, M.-C. Yen, C.-J. Lee, Y.-J. Lee and W.-C. Lin, ACS Applied Nano Materials 6 (16), 14841-14848 (2023).

# Raman and ARPES Characterization of Black Phosphorus for Contact Metal Optimization in FET Devices

**Shuo-Cheng Tsao, Shih-Po Chien, Yann-Wen Lan**

Department of Physics, National Taiwan Normal University  
e-mail: stu1051011@gmail.com



## ABSTRACT

Black phosphorus (BP) is a two-dimensional semiconductor with a low band gap (0.3–1.5 eV) and bipolar transport characteristics. Its conduction type can be modulated by selecting different contact metals, enabling diverse electronic applications[1], [2]. In this study, BP was characterized using Raman spectroscopy[3] and ARPES[4]. FET devices with various metal contacts were fabricated via photolithography, and their electrical behavior was measured. The aim is to identify the optimal contact metal and protective layer combination for the best device performance.

## References

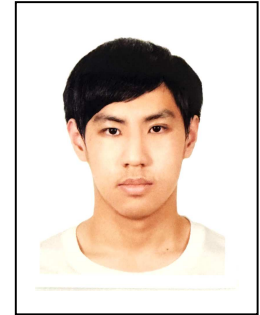
- [1] Yu. Yu. Illarionov *et al.*, “Highly-stable black phosphorus field-effect transistors with low density of oxide traps,” *NPJ 2D Mater Appl*, vol. 1, no. 1, p. 23, 2017, doi: 10.1038/s41699-017-0025-3.
- [2] L. Liu *et al.*, “Scalable Van der Waals Encapsulation by Inorganic Molecular Crystals,” *Advanced Materials*, vol. 34, no. 7, p. 2106041, Feb. 2022, doi: <https://doi.org/10.1002/adma.202106041>.
- [3] S. Liang, M. N. Hasan, and J.-H. Seo, “Direct Observation of Raman Spectra in Black Phosphorus under Uniaxial Strain Conditions,” *Nanomaterials*, vol. 9, no. 4, 2019, doi: 10.3390/nano9040566.
- [4] C. Q. Han *et al.*, “Electronic structure of black phosphorus studied by angle-resolved photoemission spectroscopy,” *Phys Rev B*, vol. 90, no. 8, p. 85101, Aug. 2014, doi: 10.1103/PhysRevB.90.085101.



# Interface Trap Reduction and Channel Optimization in 2D FETs through Dielectric and Work Function Engineering

**Shih-Chia Peng<sup>†</sup>, You-Jia Huang, Tater Jyoti,  
Joy-Yi Fu, Yann-Wen Lan\***

National Taiwan Normal University, department of physics, ASQNL  
e-mail: 41141208S@gapps.ntnu.edu.tw



## ABSTRACT

Two-dimensional (2D) materials have emerged as promising candidates for addressing short-channel effects in advanced field-effect transistors (FETs). However, interface traps between the dielectric layer and the semiconductor channel can significantly degrade device performance by influencing subthreshold swing and inducing hysteresis loop. In this work, we present the fabrication and optimization of 2D-material-based FETs employing antimony oxide ( $\text{Sb}_2\text{O}_3$ ) as a high-k, van der Waals (vdW) dielectric<sup>1</sup>. Our experimental results demonstrate that controlled annealing during the deposition process reduces gate leakage currents, improves the on/off ratio, and lowers the interface trap density ( $D_{it}$ ), thereby enhancing overall device reliability. Furthermore, we investigate metal work function modulation as a strategy to achieve enhanced p-type behavior, along with efforts to realize transfer-free processing for improved structural integrity and scalability. Given the growing relevance of 2D FETs in applications such as logic circuits and memory, this study lays foundational insights for scalable and low-defect integration of 2D semiconductors with vdW-compatible high-k dielectrics in advanced nanoelectronics.

## References

1. Liu, K., Jin, B., Han, W. *et al.* A wafer-scale van der Waals dielectric made from an inorganic molecular crystal film. *Nat Electron* **4**, 906–913 (2021).  
<https://doi.org/10.1038/s41928-021-00683-w>

# Enhanced Synaptic Memory Window and Linearity with Laguerre-Gaussian Beam

**Wei-Cheng Chen<sup>1</sup>, Shih-Po Chien<sup>1</sup>, Jung-Yao Chen<sup>2</sup>, Yann-Wen Lan<sup>1</sup>**

Affiliation: <sup>1</sup>Department of Physics, National Taiwan Normal University, Taipei 116, Taiwan.

<sup>2</sup>Department of Photonics, National Cheng Kung University, Tainan 701, Taiwan.

e-mail: weichenghwsh416@gmail.com



## ABSTRACT

Synaptic memory devices are seen as a promising candidate for neuromorphic computing (NC) and can contribute multilevel memory states that are essential for emulating analog synaptic weights in ANNs. Herein a gated 3-terminal (3T) nonvolatile opto-memtransistor is demonstrated, based on pentacene/polystyrene-*block*-poly(ethylene oxide) (PS-*b*-PEO)/(4-Biphenylmethylammonium)<sub>2</sub>ZnI<sub>4</sub> (BPMA)<sub>2</sub>ZnI<sub>4</sub> composite. The PS-*b*-PEO/(BPMA)<sub>2</sub>ZnI<sub>4</sub> layer functions as charge storage medium and photoactive gate and the pentacene is the active channel. In this work, the device exhibited dual-mode memory behavior in which both the gate and source-drain channel contribute memory functionality under the electrical field. We stimulated the photoactive layer the Laguerre-Gaussian (LG) beams carrying orbital angular momentum (OAM) with the azimuthal index (or topological charge  $\ell$ ) ranging from 0 to 5. A threshold voltage ( $V_{th}$ ) was found to shift from -15 V to +15 V, confirming that LG beams can effectively induce photowriting and expand the memory window. Post-illumination measurements revealed significantly improved linearity in both potentiation and depression processes, suggesting that OAM light can optimize synaptic memory performance. Future work suppose focus on the relation of the topology charge and memory functionality. This study represents a state-of-the-art for the neuromorphic computing and reveals the new avenues for topology-driven optoelectronic memory .

## References

1. Jung-Yao Chen, Yu-Cheng Chiu, Yen-Ting Li, Chu-Chen Chueh, and Wen-Chang Chen, **Nonvolatile Perovskite-Based Photomemory with a Multilevel Memory Behavior**, *Adv. Mater.*, 29, 1702217 (2017).
2. Zhu, K., Zhang, F., & Kim, **3D/2D Multidimensional Perovskites: Balance of High Performance and Stability for Perovskite Solar Cells**, *Current Opinion in Electrochemistry*, 11, 105-113 (2018).

# Exploring Dark Exciton in WSe<sub>2</sub> Through Orbital Angular Momentum Light

**Yi-Chun Chen, Ye-Ru Chen, Yann-Wen Lan**

Department of Physics, National Taiwan Normal University

e-mail: 41141203S@gapps.ntnu.edu.tw



## ABSTRACT

The presence of strong spin-orbit coupling in the valence band and weak spin-splitting in the conduction band results in the lowest energy exciton in WX<sub>2</sub> (X = S, Se) being spin forbidden and optically dark. Because of their long lifetimes, dark excitons are highly attractive for quantum optics and optoelectronic applications.<sup>1</sup> Based on the theoretical calculations related to dark excitons, it has been found that a substantial enhancement of the photoexcitation of gray excitons (GXs), a type of spin-forbidden dark exciton (DX), in a WSe<sub>2</sub> monolayer (ML) can be achieved through the utilization of a 3D-structured twisted light with the optical spin-orbit interaction.<sup>2</sup> Accordingly, this study aims to observe dark excitons in WSe<sub>2</sub> by employing light carrying orbital angular momentum (OAM). To further enhance the excitonic signals, we also reduce the sample temperature and apply polarization to the incident beam.

## References

1. M. Rahaman, O. Selyshchev, Y. Pan, R. Schwartz, I. Milekhin, A. Sharma, G. Salvan, S. Gemming, T. Korn, D. R. T. Zahn, **Adv. Optical Mater.**, 2021, 9, 2101801
2. O. J. G. Sanchez, G. H. Peng, W. H. Li, C. H. Shih, C. H. Chien, S. J. Cheng, **ACS Nano**, 2024, 18, 17, 11425–11437
3. R. Kesarwani<sup>1</sup>, K. B. Simbulan, T. D. Huang, Y. F. Chiang, N. C. Yeh, Y. W. Lan, T. H. Lu, **Sci. Adv.** **8**, eabm0100 (2022)

# Pressure-Tunable Magnetism in 2D Ferromagnetic $\text{Fe}_3\text{GaTe}_2$ via Local AFM Indentation

**Hsin-Sung Chen, Ming-Hsien Hsu, Wen-Chin Lin\***

Department of Physics, National Taiwan Normal University

e-mail: wclin@ntnu.edu.tw

Paste your  
photo here

## ABSTRACT

The discovery of two-dimensional ferromagnetic van der Waals materials has opened a wide array of novel research opportunities in materials science. Recently, studies have shown that the exchange interactions and magnetocrystalline anisotropy of  $\text{Fe}_3\text{GaTe}_2$  (FGaT) are highly sensitive to applied pressure. Another study has reported that pressure can induce a phase transition in  $\text{Fe}_3\text{GaTe}_2$  from a ferromagnetic (FM) to an antiferromagnetic (AFM) state. Under such conditions, partial regions of FGT undergo this transition, leading to the formation of FM/AFM heterointerfaces and the emergence of an exchange bias (ExB) effect. Moreover, pressure has been found to significantly enhance the perpendicular magnetic anisotropy (PMA) of  $\text{Fe}_3\text{GaTe}_2$  (FGaT) and increase its anomalous Hall effect (AHE). These findings suggest that pressure is an effective approach for tuning the magnetic properties of two-dimensional ferromagnetic van der Waals materials, thereby expanding their potential for diverse applications.

In this study, we applied localized pressure to FGaT using an atomic force microscope (AFM) and monitored the resulting magnetic changes via the magneto-optical Kerr effect (MOKE). Our preliminary results indicate that even localized pressure can influence the overall magnetic response of FGaT, rather than altering only the region under direct mechanical stress. This behavior appears to be independent of the sample thickness. Furthermore, we observed a clear trend of decreasing coercive field following the application of pressure.

## References

1. Wang, Heshen, et al. "Pressure-dependent intermediate magnetic phase in thin  $\text{Fe}_3\text{GaTe}_2$  flakes." *The Journal of Physical Chemistry Letters* 11.17 (2020): 7313-7319.
2. Liu, Caixing, et al. "Emergent, Non-Aging, Extendable, and Rechargeable Exchange Bias in 2D  $\text{Fe}_3\text{GaTe}_2$  Homostructures Induced by Moderate Pressuring." *Advanced Materials* 35.1 (2023): 2203411.
3. Iimori, Riku, et al. "Substantial enhancement of perpendicular magnetic anisotropy in van der Waals ferromagnetic  $\text{Fe}_3\text{GaTe}_2$  film due to pressure application." *Communications Materials* 5.1 (2024): 235.

# Photoluminescence of MoS<sub>2</sub> on Platinum Substrate

## Tzu-Han Chang, Asha Yadav, Yu-Chen Chang, Ting-Hua Lu

Department of Physics, National Taiwan Normal University  
e-mail: b0935582248@gmail.com



## ABSTRACT

Based on our previous research, we found that monolayer MoS<sub>2</sub> on a Pt/SiO<sub>2</sub>/Si substrate shows a blue shift and enhanced photoluminescence (PL) intensity under both polarized and unpolarized light. In this study, we further explore the effects of dense array patterns on the Pt substrate to understand how they influence the optical properties and polarization behavior of MoS<sub>2</sub> emission. This extended research aims to provide new material strategies for future optoelectronic device applications.

## References

1. Wang et al., Nanophotonics, 10(6), 1733–1740 (2021).
2. Wen et al., Science Advances, 6(7), eaba1234 (2020).

# Photoresponse and Trap-State Effects in Monolayer MoS<sub>2</sub> Phototransistors Under Low-Power Illumination

**Shuo-Yu Tseng<sup>†</sup>, Shih-Chia Peng , Yann-Wen Lan and  
Ting-Hua Lu**

Department of Physics, National Taiwan Normal University  
e-mail: 41141222S@gapps.ntnu.edu.tw

## ABSTRACT

We investigate the photoresponse behavior of monolayer molybdenum disulfide (MoS<sub>2</sub>) phototransistors fabricated via chemical vapor deposition (CVD) in a back-gated field-effect transistor configuration. Under low-power 532 nm laser illumination, the photocurrent exhibits a sublinear dependence on optical power, with a fitted power-law exponent of  $\alpha \approx 0.36$ , indicating a dominant influence from surface trap states and carrier recombination. The device achieves a responsivity of 2.19 A/W at 5  $\mu$ W, which decreases significantly with increasing optical power, suggesting that trap saturation reduces photoresponse efficiency. This behavior aligns with trap-assisted photogating mechanisms reported in the literature and highlights the surface sensitivity of monolayer MoS<sub>2</sub> optoelectronic properties. Future work will include time-resolved measurements and gate-dependent photoresponse analysis to further elucidate the role of trap occupation and carrier transport. These findings enhance our understanding of trap-dominated photoresponse in two-dimensional semiconductors and their potential for low-light detection applications.

## References

1. Y. Li, L. Li, S. Li, J. Sun, Y. Fang, T. Deng, *ACS Omega* **7**, 38315–38323 (2022).
2. A. Di Bartolomeo, L. Genovese, F. Giubileo, T. Foller, M. Schleberger, L. Lemmo, *Nanotechnology* **28**, 214002 (2017)



# Emission Current Stability of Single-Atom Electron Sources

C.-T. Wu<sup>1,2</sup>, T.-Y. Fu<sup>2</sup> and I.-S. Hwang<sup>1</sup>

<sup>1</sup> *Institute of Physics, Academia Sinica, Taipei, Taiwan*

<sup>2</sup> *Department of physics, National Taiwan Normal University, Taipei, Taiwan*

E-mail: shinaarika1229@gmail.com



The most important characteristics of an electron emission source are brightness, coherence, and current stability. Among conventional electron emitters, cold field emission offers the highest brightness, with further advancements seen in nanotip and single-atom tip (SAT) designs. While single-atom emitters (often formed by combining a single atom on a sharp tip) generally exhibit superior coherence, they often suffer from a lack of stable current emission.

In 2001, Fu et al. developed the first Pd-covered W(111) SAT covered Pd monolayer evaporation and annealing in UHV, inspired by Madey's work [1]. These SATs are stable W(111) nanopyramids covered with noble-metal atoms, regenerable by annealing. Kuo et al. developed an electroplating method to create noble metal-covered W(111) SATs. These regenerable pyramidal tips, structurally identical to Fu's, are formed by annealing plated tips, and can withstand numerous regenerations after damage [2]. Our SAT offers minimal source size ( $2^\circ$  half angle), high coherence, and superior brightness. This enhances electron microscope speed and S/N ratio. Its optimal coherence yields diffraction signals crucial for observing graphene contaminants and performing CDI to reconstruct 2D material structures and defects.

The potential of pyramid structure SATs as an ideal electron emitter has been further substantiated by rigorous experimental investigations. Ishikawa et al. developed that the Pd-covered tip was applied to an emission gun system. It was found that the ratio of total to probe current was 80%, indicating only a 20% decrease in emission current [3]. The achieved brightness of  $10^{10}$  A/cm<sup>2</sup> sr at 2 keV is thousands of times higher than that of traditional electron emission gun source.

In our study, we prepared different radii of curvature (ROC). These tips were electrochemically coated with palladium, and SATs were grown in an ultrahigh vacuum ( $< 3 \times 10^{-8}$  Pa). Emission probe current was measured by Faraday cup. According to our research, a ROC 300 nm tip can stably emit a maximum of 1 nA, whereas a ROC 40 nm tip can stably emit a maximum of 500 pA for a few hours during our observation. In future work, we will use different noble metals to cover the W(111) surface and measure the emission current.

[1] T.-Y. Fu *et al.* Phys. Rev.B: Condens. Matter Mater. Phys., 64, 113401 (2001)

[2] H.-S. Kuo *et al.* Nano Lett., 4, 2379–2382 (2004)

[3] T. Ishikawa *et al.* Appl. Phys. Lett. 90, 143120 (2007)

# Effects of Dielectric Mismatch-Induced Lateral Heterojunctions and Annealing on the Optical Properties of WS<sub>2</sub>

**Jui-Po Chen<sup>1</sup>, Yann-Wen Lan<sup>1</sup>, Jan-Chi Yang<sup>2</sup>, Ting-Hua Lu<sup>1</sup>**

<sup>1</sup>Department of Physics, National Taiwan Normal University, Taipei, Taiwan

<sup>2</sup>Department of Physics, National Cheng Kung University, Tainan, Taiwan

e-mail: 41141121s@gapps.ntnu.edu.tw

## ABSTRACT

Atomically thin transition metal dichalcogenides (TMDs) have attracted significant attention in optoelectronics due to their unique bandgap characteristics. Owing to their low dimensionality, TMDs are highly susceptible to external perturbations, making substrate engineering an effective strategy for tuning their properties. Recent studies have shown that when TMDs are placed at the interface between two materials with significantly different dielectric constants. Their band structure can be modified by the substrate-induced potential, forming a PN junction and exhibiting diode-like behavior<sup>1</sup>.

In this study, we investigate the optical properties of tungsten disulfide (WS<sub>2</sub>), a representative semiconducting TMD, transferred across the boundary between FS-STO and Si/sapphire substrates. The dielectric mismatch between the two substrates induces lateral heterojunctions that modulate the bandgap of WS<sub>2</sub>. We systematically examine the photoluminescence (PL) spectra, PL lifetimes, and degree of circular polarization (DoCP) of WS<sub>2</sub> on different substrates and at different locations, in order to explore how the PN junction-like band modulation and the high-dielectric environment influence its optical response. In addition, we investigate the effects introduced by post-annealing treatments.

Our results show that the presence of FS-STO suppresses the PL intensity of WS<sub>2</sub> and causes instability in its PL lifetime. Conversely, annealing leads to reduced PL lifetimes on sapphire substrates but results in an opposite trend on Si substrates.

These findings shed light on how high-dielectric-defined lateral heterojunctions influence the band structure and optical characteristics of 2D semiconductors. This study highlights the potential of dielectric interface engineering for advancing applications of two-dimensional materials in optoelectronics and spintronics.

## References

1. Utama, M.I.B., Kleemann, H., Zhao, W. *et al.* **A dielectric-defined lateral heterojunction in a monolayer semiconductor.** *Nat Electron* **2**, 60–65 (2019).

# Mapping Local Electrochemical Responses of 2D TMDCs Using AFM-SECM

**Sumangaladevi Koodathil<sup>1,2,3,4\*</sup>, Mohammad Qorbani<sup>4</sup>,  
Septia Kholimatussadiah<sup>4,5</sup>, Sankar Raman<sup>6</sup>, Li-Chyong  
Chen<sup>4,5</sup>, and Kuei-Hsien Chen<sup>3,4</sup>**



*1Molecular Science and Technology Program, Taiwan International Graduate Program, Academia Sinica, Taipei 10617, Taiwan*

*2International Graduate Program of Molecular Science and Technology, National Taiwan University, Taipei 10617, Taiwan*

*3Institute of Atomic and Molecular Sciences, Academia Sinica, Taipei 10617, Taiwan*

*4Center for Condensed Matter Sciences, National Taiwan University, Taipei 10617, Taiwan*

*5Department of Physics, National Taiwan University, Taipei, Taiwan*

*6Institute of Physics, Academia Sinica, Taipei, Taiwan*

*\*Email: suma.parappa@gmail.com*

## ABSTRACT

Transition metal dichalcogenides (TMDCs) are emerging as promising materials for renewable energy applications due to their unique electronic properties and abundance. However, their electrocatalytic performance is significantly influenced by interfacial factors such as electron transfer kinetics, surface morphology, and strain etc. This study utilizes scanning electrochemical microscopy (SECM) in coupled with atomic force microscopy (AFM) to investigate the local electrocatalytic activity of 2D TMDCs (MoS<sub>2</sub> & WSe<sub>2</sub>). Mapping the electrochemical response and surface topography by AFM-SECM feedback mode, we reveal layer-dependent activity, strain-induced changes, and the impact of doping and heterostructure formation. AFM-SECM feedback mapping demonstrates the layer-dependent electrocatalytic ability of MoS<sub>2</sub> to oxidize the redox species Ru<sup>2+</sup> back to Ru<sup>3+</sup>. The electrocatalytic activity and electron transfer efficiency increase with the layer thickness of MoS<sub>2</sub>, and wrinkled regions of the MoS<sub>2</sub> flakes exhibit higher feedback currents, likely due to enhanced surface reactivity and strain-induced electronic effects. The electrochemical activity of vanadium-doped MoS<sub>2</sub> thin films is significantly higher than that of pristine MoS<sub>2</sub>, as observed through mapping and tip-surface distance curve. Furthermore, Kelvin probe force microscopy (KPFM) is employed to visualize surface potential variations, providing insights into the electronic structure and charge distribution within the TMDC materials. Our findings offer valuable guidance for the rational design and optimization of TMDC-based electrocatalysts, paving the way for more efficient and sustainable energy conversion systems.

## References

1. Du, HY. et al. Nat Commun 12, 1321 (2021).
2. Qorbani, M. et al. Nat Commun 13, 1256 (2022).
3. Si Keyu. et al. Applied Surface Science, Volume 507, 145082 (2020)

# Harnessing Non-Hermiticity for Fast GHZ- and W-state Generation in Superconducting Qubits

**C. G. Feyisa<sup>1, 2, 3</sup>, J. S. You<sup>4</sup>, H. Y. Ku<sup>4</sup>, and H. H. Jen<sup>1, 2, 5</sup>**

<sup>1</sup> *Institute of Atomic and Molecular Sciences, Academia Sinica, Taipei 10617, Taiwan*

<sup>2</sup> *Molecular Science and Technology, Taiwan International Graduate Program, Academia Sinica, Taipei 10617, Taiwan*

<sup>3</sup> *Department of Physics, National Central University, Taoyuan 320317*

<sup>4</sup> *Department of Physics, National Taiwan Normal University, Taipei 11677, Taiwan*

<sup>5</sup> *Physics Division, National Center for Theoretical Sciences, Taipei 10617, Taiwan*

## ABSTRACT

Parity-time ( $\mathcal{PT}$ )-symmetric non-Hermitian systems exhibit unique spectral singularity known as exceptional points (EPs), where both eigenvalues and eigenvectors coalesce. These EPs are essential for quantum control, and allow fast and robust quantum state engineering that surpasses the performance of conventional Hermitian quantum systems. Harnessing these unique non-Hermitian features, we theoretically investigate multipartite entanglement dynamics in non-Hermitian superconducting qubits with flexible coupling topologies and in the hybrid non-Hermitian and Hermitian regime. We show that non-Hermitian qubits with all-to-all coupling generate GHZ states, while those with nearest-neighbor interactions favor the formation of W-state. These entangled states remain robust against coupling asymmetries, off-resonant driving errors, and decoherence effects stemming from quantum jumps. Moreover, the hybrid architecture allows dynamical switching between distinct entangled states. We further show that our results remain valid under strong coupling regimes and are scalable to larger system sizes. These findings reveal that exploiting non-Hermitian systems and their associated exceptional points supports robust and genuine entangled state preparation with applications in both foundational quantum research and emerging quantum technologies.

## References

1. C. G. Feyisa, J. S. You, H. Y. Ku, and H. H. Jen **Quantum Sci. Technol.** *10*, 025021- (2025).
2. C. G. Feyisa, C. Y. Liu, M. S. Hasan, J. S. You, H. Y. Ku, and H. H. Jen **arXiv:2411.17457**. (2024).



## Effect of Defects on Electronic and Magnetic Properties in NiPS<sub>3</sub> Layers

**Pritam Sardar, Sheng-Chieh Huang, Chao-Cheng Kaun**

Department of Physics, National Central University  
Molecular Science and Technology Program, Taiwan International Graduate Program,  
Academia Sinica and National Central University  
Research Center for Applied Sciences, Academia Sinica  
e-mail: sardar0001@as.edu.tw

### ABSTRACT

MPX<sub>3</sub> (M = transition metal, X = chalcogen) are new class of extensively studied materials due to their profound applications in magneto-optic, magnetic storage, high temperature superconductivity, and 2D magnetism. Particularly NiPS<sub>3</sub> has a high Neel temperature (T<sub>N</sub>) of ~ 155 K. But very few studies have been conducted on the effects of defects on NiPS<sub>3</sub>. Our simulations using Density-Functional-Theory (DFT) leads to a band gap of ~ 1.68 eV and 1.78 eV for bulk and monolayer phase with a stable zig-zag anti-ferromagnetic (AFM) ground state. Our study of strain has shown that defect engineering is a crucial tool to alter and understand the magnetic configuration of NiPS<sub>3</sub>. Our study will further motivate to find applications of NiPS<sub>3</sub> layers in more advanced and exotic topics like superconductivity and skyrmions.

### References

1. Chittari, Bheema Lingam et al. (2016). "Electronic and magnetic properties of singlelayer MPX<sub>3</sub> metal phosphorous trichalcogenides". In: Physical Review B 94.18, p. 184428.
2. Wang, Fengmei et al. (2021). "Defect-mediated ferromagnetism in correlated twodimensional transition metal phosphorus trisulfides". In: Science Advances 7.43, eabj4086.

# Absolute Line Strength Measurements of HO<sub>2</sub> $\nu_1$ and $\nu_2$ Fundamental Bands

**Che-Wei Chang<sup>a,b,c</sup>, I-Yun Chen<sup>a,d</sup>, Qian-Rui**

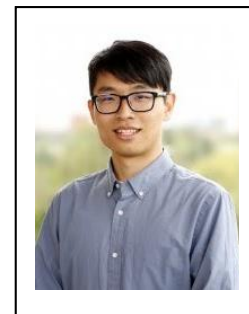
**Huang<sup>a</sup>, Jer-Lai Kuo<sup>a</sup>, Pei-Ling Luo<sup>\*a</sup>**

<sup>a</sup> Institute of Atomic and Molecular Sciences Academia Sinica, Taipei 106319, Taiwan.

<sup>b</sup> Molecular Science and Technology Program, Taiwan International Graduate Program, Academia Sinica, 11529, Taipei, Taiwan.

<sup>c</sup> International Graduate Program of Molecular Science and Technology, National Taiwan University, 10617, Taipei, Taiwan.

<sup>d</sup> Department of Chemistry, National Taiwan University, Taipei 10617, Taiwan.  
e-mail: victorchang12323@gmail.com



## ABSTRACT

Hydroperoxyl radical (HO<sub>2</sub>) is one of the most important oxidizing species in tropospheric chemistry [1]. In this work, the absolute line strengths of HO<sub>2</sub> in the  $\nu_1$  and  $\nu_2$  fundamental bands were determined using synchronized two-color time-resolved dual-comb spectroscopy [2,3]. HO<sub>2</sub> was generated via laser photolysis of a flowing Cl<sub>2</sub>/CH<sub>3</sub>OH/O<sub>2</sub> gas mixture. By simultaneously probing HO<sub>2</sub> in 7.1  $\mu\text{m}$  and its byproduct, HCl, in 3.3  $\mu\text{m}$ , the absolute line strengths of the HO<sub>2</sub>  $\nu_2$   $7_{1,6} \leftarrow 6_{1,5}$  F<sub>1,2</sub> transitions at 1407.620 cm<sup>-1</sup> were determined with an uncertainty of 4.9% referenced to the accurately known R(9) transition of HCl. Additionally, line strengths for several HO<sub>2</sub> transitions in the  $\nu_1$  band (2.9  $\mu\text{m}$ ) were determined based on the simultaneously probed  $\nu_2$   $7_{1,6} \leftarrow 6_{1,5}$  F<sub>1,2</sub> transitions (7.1  $\mu\text{m}$ ) or  $\nu_3$   $13_{1,13} \leftarrow 12_{1,12}$  F<sub>1,2</sub> transitions (8.9  $\mu\text{m}$ ). With the obtained absolute line strengths and by spectral analysis using PGOPHER, the band strengths for  $\nu_1$  and  $\nu_2$  fundamental bands were determined to be 18.5 $\pm$ 1.5 km mol<sup>-1</sup> and 26.6 $\pm$ 1.3 km mol<sup>-1</sup>, respectively. This work provides precisely measured line strengths of HO<sub>2</sub> useful in field measurements and essential updated spectroscopic data to support future revisions of current databases.

## References

1. D. Stone, L. K. Whalley, and D. E. Heard. **Chem. Soc. Rev.**, *41*, 6348–6404 (2012).
2. I-Y. Chen, C.-W. Chang, Q.-R. Huang, J.-L. Kuo, P.-L. Luo. **Phys. Chem. Chem. Phys.** (in Review).
3. C.-W. Chang, I-Y. Chen, and P.-L. Luo. **J. Chem. Phys.**, *162*, 034302 (2025).



# Tuning the selectivity of Electrocatalytic CO<sub>2</sub> Reduction by Engineering the Coordination Environment of Bi SACs

**Varad A. Modak<sup>1,2,3</sup>, Osama Nasr<sup>1,4,5,6,7</sup>, Li-Chyong Chen<sup>4,8</sup> and Kuei-Hsien Chen<sup>1,4\*</sup>**

<sup>1</sup> Institute of Atomic and Molecular Sciences, Academia Sinica, Taipei 10617, Taiwan

<sup>2</sup> International Graduate Program of Molecular Science and Technology, National Taiwan University (NTU-MST), Taipei 10617, Taiwan

<sup>3</sup> Molecular Science and Technology Program, Taiwan International Graduate Program (TIGP), Academia Sinica, Taipei 11529, Taiwan

<sup>4</sup> Center for Condensed Matter Sciences, National Taiwan University, Taipei 10617, Taiwan

<sup>5</sup> Sustainable Chemical Science and Technology, Taiwan International Graduate Program, Academia Sinica, Nankang, Taipei 11529, Taiwan

<sup>6</sup> Institute of Chemistry, Academia Sinica, Nankang, Taipei 11529, Taiwan

<sup>7</sup> Department of Applied Chemistry, National Yang Ming Chiao Tung University, Hsinchu 30010, Taiwan

<sup>8</sup> Center of Atomic Initiative for New Materials, National Taiwan University, Taipei 10617, Taiwan

\*Email: vmodak97@gmail.com

## ABSTRACT

This project is centred on the development of Bismuth-based single-atom catalysts (Bi-SACs) supported on structurally tuneable nitrogen-doped carbon (NC) frameworks for the electrochemical reduction of carbon dioxide (CO<sub>2</sub>). By leveraging the atomic dispersion of Bi on engineered NC supports, the goal is to construct active sites with well-defined coordination environments that promote selective conversion of CO<sub>2</sub> <sup>[1]</sup>. Single-atom configurations are particularly attractive due to their high atom utilization, unique electronic properties, and ability to avoid bulk metal aggregation that often leads to reduced selectivity.

Initial performance evaluations reveal a promising catalytic profile, yielding formic acid as the sole liquid product with a high Faradaic efficiency (FE). Hydrogen is observed as the dominant gas-phase byproduct, with only minor amounts of carbon monoxide detected. However, in a parallel case, formic acid was obtained in reduced amounts, with CO being the dominant gaseous product with the balance made up by H<sub>2</sub>. These results demonstrate a relatively clean product distribution, yet leave room for optimization—especially in reducing the competitive hydrogen evolution reaction (HER), which limits formic acid selectivity. It is also of academic and practical interest, to investigate how the NC support influences the selectivity <sup>[2]</sup>.

The central aim of this work is to fine-tune both the catalyst and the NC support to achieve a simplified and efficient product distribution. Emphasis is placed on increasing the throughput and selectivity toward formic acid without sacrificing catalyst stability or scalability. Key strategies include optimizing synthesis parameters to precisely control Bi atom dispersion and coordination, and the introduction of inhomogeneous coordination to achieve the desired catalysis goal.

Through these efforts, the project seeks to enhance the efficiency and sustainability of CO<sub>2</sub> electroreduction, contributing to carbon-neutral chemical manufacturing. This work not only provides insight into the structure–function relationship of single-atom catalysts but also presents a viable pathway for practical, scalable formic acid production from CO<sub>2</sub> under ambient conditions.

## References:

- 1) Santra, S., Streibel, V., Wagner, L. I., Cheng, N., Ding, P., Zhou, G., ... & Sharp, I. D. (2024). Tuning Carbon Dioxide Reduction Reaction Selectivity of Bi Single-Atom Electrocatalysts with Controlled Coordination Environments. *ChemSusChem*, 17(10), e202301452.
- 2) Zhu, M. N., Jiang, H., Zhang, B. W., Gao, M., Sui, P. F., Feng, R., ... & Luo, J. L. (2023). Nanosecond laser confined bismuth moiety with tunable structures on graphene for carbon dioxide reduction. *ACS nano*, 17(9), 8705-8716.

# **Modulatable melanocyte dedifferentiation through niche prolactin sensing controls seasonal coat color switch in Djungarian hamster**

**Yu-Sheng Yu<sup>1</sup> , Shin-Kuo Chen<sup>2</sup> ,Yi-Chun Wu<sup>1,3</sup>, Sung-Jan Lin<sup>1,4</sup>**

1 Molecular Science and Technology, Taiwan International Graduate Program, and National Taiwan University

2 Department of Life Science, National Taiwan University, Taipei, Taiwan

3 Institute of Molecular and Cellular Biology, National Taiwan University, Taipei, Taiwan

4 Department of Biomedical Engineering, National Taiwan University, Taipei, Taiwan

## **Abstract**

Circannual coat color switch for camouflage provides survival advantage in polar animals. Systemic prolactin levels, lower in short photoperiods (SP), have been shown to control the color switch, but little is known about the underlying regulatory mechanisms. We found that, in Djungarian hamsters (*Phodopus sungorus*), hair regenerated in SP showed a longer distal depigmented stretch caused by prolonged halt of melanin production, generating a white coat. Mechanistically, prolactin is sensed by hair follicle dermal papilla fibroblasts and low prolactin levels in SPs prolongedly suppress their endothelin 3 (EDN3) secretion. Without paracrine EDN3 signaling, adjacent melanocytes revert to a stem cell state and stop melanin production. We also found that prolactin production is controlled by duration of nocturnal activity but no total daily ambient light exposure. Longer nocturnal activity suppresses pituitary prolactin secretion by increasing dopamine-producing cells in paraventricular nuclei through enhancing the release of (CCK, etc.) from suprachiasmatic nuclei. Our work demonstrates neural networks that regulate prolactin production and a peripheral prolactin-responsive system for seasonal coat color switch. Analogous mechanisms might also operate in other organs with circannual changes.

# Exploring the influence of S/Cl sites' mixing on the lithium diffusion behaviors of $\text{Li}_{x+6}\text{PS}_4(\text{S/Cl})$



**Lily M Angraini<sup>1,2,3</sup>, Cheng-Rong Hsing<sup>4</sup>, Ching-Ming Wei<sup>3,5</sup>**

<sup>1</sup>International Graduate Program of Molecular Science Technology (NTU-MST), National Taiwan University, No. 1, Sec. 4, Roosevelt Road, Taipei 10617, Taiwan

<sup>2</sup>Taiwan International Graduate Program (TIGP), Academia Sinica No. 128, Sec. 2 Academia Road, Taipei 11529, Taiwan

<sup>3</sup>Institute of Atomic and Molecular Sciences, Academia Sinica, Taipei 10617, Taiwan

<sup>4</sup>Division of Natural Science, Center for General Education, Chang Gung University, Taoyuan City, 33302, Taiwan

<sup>5</sup>Institute of Physics, Academia Sinica, Nankang 11529, Taiwan

[cmw@phys.sinica.edu.tw](mailto:cmw@phys.sinica.edu.tw), [lilyangraini@unram.ac.id](mailto:lilyangraini@unram.ac.id)

## ABSTRACT

Due to its exceptionally high ionic diffusion dynamics and stability, the compound  $\text{Li}_{6+x}\text{PS}_4(\text{S/Cl})$ , lithium argyrodite, has demonstrated significant potential as an electrolyte in solid-state batteries. Structural mixing of S/Cl at Wyckoff's sites found by experimental XRD is expected to significantly affect the Li ions' movements through this material; however, it needs to be determined and answered how this mixing affects lithium diffusion and its correlation with the diffusion coefficients. In this work, we perform large-scale molecular dynamics simulations on  $\text{Li}_{6+x}\text{PS}_4(\text{S/Cl})$  based on machine-learning interatomic potentials fitted from ab initio molecular dynamics simulations. We carefully study the influence of Li-ion concentrations as well as S/Cl site mixing on lithium diffusion behaviours in  $\text{Li}_{6+x}\text{PS}_4(\text{S/Cl})$ . The results indicate that an increase or decrease in the concentration of lithium (Li) away from  $\text{Li}_{6+x}\text{PS}_4(\text{S/Cl})$ , or S/Cl sites' mixing, can increase the diffusion coefficient by one to two orders of magnitude from  $10^{-7}$  to  $10^{-5}$   $\text{cm}^2/\text{s}$  and increase the ionic conductivity by one order of magnitude, from  $10^{-2}$  to  $10^{-1}$   $\text{S/cm}$ . Furthermore, the Arrhenius equation can describe the diffusion behaviour of lithium atoms well, where the activation barrier ranges from 108 to 187 meV with a strong dependence on lithium concentrations and S/Cl site mixing configurations. The small diffusion barriers provide the fundamental origin for the fast diffusion behaviours of lithium atoms. Moreover, the calculated ion conductivity values are an order of magnitude higher than the experimental results, which typically range between  $10^{-3}$  to  $10^{-2}$   $\text{S/cm}$ , where the discrepancies might be attributed to the structural difference between idealized computational models and imperfect experimental structures with various types of defects.

## References

1. Z. Dheng, Z. Zhu, I.H.Chu, S.P.Ong, **Chem. Matter**, Data-Driven First-Principles Methods for the Study and Design of Alkali Superionic Conductors, 29, 281-288. (2017).
2. A. Baktash, J.C.Reid, T.Roman, D.J.Searles, **Nature Computational Material**, Diffusion of lithium ions in Lithium-argyrodite solid-state electrolytes, 162, (2020)
3. R. Schelenker, A.Hansen, et al. **Chem. Matter**. Structure and diffusion pathways in  $\text{Li}_6\text{PS}_5\text{Cl}$  argyrodite from neutron diffraction, pair-distribution function analysis, and NMR, 32, 8420–8430, (2020).
4. Novikov, I. S., Gubaev, K., Podryabinkin, E. V & Shapeev, A. V. *Mach Learn Sci Technol* **2**, 025002 (2021).
5. Podryabinkin, E. V. & Shapeev, A. V. *Comput Mater Sci* **140**, 171–180 (2017).

# Suppression of quantum correlations in a clean-disordered atom-nanophotonic interface

**I Gusti Ngurah Yudi Handayana<sup>1,2,3,\*</sup>, Yi-Lin Tsao<sup>3,4</sup>, and H. H. Jen<sup>3,1,5,†</sup>**

<sup>1</sup>Molecular Science and Technology Program, Taiwan International Graduate Program, Academia Sinica, Taiwan

<sup>2</sup>Department of Physics, National Central University, Taoyuan City 320317, Taiwan

<sup>3</sup>Institute of Atomic and Molecular Sciences, Academia Sinica, Taipei 10617, Taiwan

<sup>4</sup>School of Physics, College of Sciences, Georgia Institute of Technology, Atlanta 30332, USA

<sup>5</sup>Physics Division, National Center for Theoretical Sciences, Taipei 10617, Taiwan  
e-mail: [ngurahyudi@unram.ac.id](mailto:ngurahyudi@unram.ac.id), [sappyjen@gmail.com](mailto:sappyjen@gmail.com)



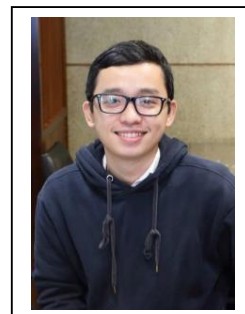
## ABSTRACT

Quantum correlations are essential to the emergent behaviors of quantum systems, supporting key phenomena such as localization or delocalization of particles, quantum avalanches in many-body localized systems, and quantum information transfer. In open atom-nanophotonic systems characterized by long-range spin-exchange interactions, we examine the influence of clean system size on high-order quantum correlations among a clean-disordered atomic array with multiple atomic excitations. By initializing the system far from equilibrium, we observe a suppression of quantum correlations for localized atomic excitations in the disordered zone as the clean system size increases, showcasing the delocalization behavior in the high-order spin-exchange processes. The calculation of the entanglement entropy at the interface further substantiates this thermalizing effect. Our results manifest distinct quantum correlations enabled by long-range interactions mediated by the waveguide, enhance the theoretical comprehension of clean-disordered systems, and provide insights to nonequilibrium quantum dynamics in an atom-nanophotonic platform.

## References

1. J. L'eonard, S. Kim, M. Rispoli, A. Lukin, R. Schittko, J. Kwan, E. Demler, D. Sels, and M. Greiner, Nat. Phys. 19, 481 (2023).
2. C.-C. Wu, K.-T Lin, I G. N. Y. Handayana, C.-H. Chien, S. Goswami, G.-D. Lin, Y.-C. Chen, and H. H. Jen, Phys. Rev. Research 6, 013159 (2024).

# Quantum-Derived Neural Network Potentials Elucidate Peptide Bond Isomerization, Charge State Stability, and Secondary Structure Distribution in Short Oligopeptides of Glycine, Alanine, and Sarcosine



**Dong Cao Hieu<sup>a,b,c</sup>, Po-Jen Hsu<sup>a</sup>, and Jer-Lai Kuo<sup>a</sup>**

a. Institute of Atomic and Molecular Sciences, Academia Sinica, Taipei, 10617, Taiwan

b. Molecular Science and Technology Program, Taiwan International Graduate Program, Academia Sinica, Taipei, 11529, Taiwan

c. International Graduate Program of Molecular Science and Technology (NTU-MST), National Taiwan University, Taipei 10617, Taiwan  
e-mail: dongcaohieu@gmail.com

## ABSTRACT

Peptide stability is fundamentally shaped by sequence length and functional group modifications. This study leverages deep learning neural network potentials (NNPs) to efficiently map the configurational landscape of neutral and zwitterionic oligopeptides (tri- to-hexa) composed of sarcosine, alanine, and glycine. The developed NNP models achieve mean absolute errors below chemical accuracy ( $\sim 4$  kcal/mol) while accelerating computations by three orders of magnitude compared to conventional ab initio methods. Our analysis reveals that cis-peptide conformers can exist within a low-energy range of 0–25 kJ/mol relative to trans conformers, with methylation significantly enhancing cis-peptide stability. Additionally, a strong positive correlation is observed between peptide chain length and the stability of zwitterionic oligosarcosine. From NNP-MD simulations of oligoalanine peptides, secondary structure analysis confirms a predominant preference for the polyproline II region, with energy uncertainties of just 3 kJ/mol, closely aligning with experimental data.